MAGNETIC RESONANCE IMAGING BASED 3D MODELS OF LEFT VENTRICULAR WALL THICKNESS AND DYSSYNCHRONY IN ACUTE MYOCARDIAL INFARCTION

AMIRAH KHALID

FACULTY OF ENGINEERING
UNIVERSITY OF MALAYA
KUALA LUMPUR

2018

MAGNETIC RESONANCE IMAGING BASED 3D MODELS OF LEFT VENTRICULAR WALL THICKNESS AND DYSSYNCHRONY IN ACUTE MYOCARDIAL INFARCTION

AMIRAH KHALID

DISSERTATION SUBMITTED IN FULFILMENT OF THE REQUIREMENTS FOR THE DEGREE OF MASTER OF ENGINEERING SCIENCE

FACULTY OF ENGINEERING
UNIVERSITY OF MALAYA
KUALA LUMPUR

2018

UNIVERSITY OF MALAYA
ORIGINAL LITERARY WORK DECLARATION

Name of Candidate: AMIRAH KHALID

Matric No: KGA160020

Name of Degree: MASTER OF ENGINEERING SCIENCE

Title of Project Paper/Research Report/Dissertation/Thesis: Assessing Regional LV Thickening Dysfunction and Dyssynchrony for Acute Myocardial Infarction.

Field of Study: BIOMEDICAL ENGINEERING

I do solemnly and sincerely declare that:

(1) I am the sole author/writer of this Work;
(2) This Work is original;
(3) Any use of any work in which copyright exists was done by way of fair dealing and for permitted purposes and any excerpt or extract from, or reference to or reproduction of any copyright work has been disclosed expressly and sufficiently and the title of the Work and its authorship have been acknowledged in this Work;
(4) I do not have any actual knowledge nor do I ought reasonably to know that the making of this work constitutes an infringement of any copyright work;
(5) I hereby assign all and every rights in the copyright to this Work to the University of Malaya ("UM"), who henceforth shall be owner of the copyright in this Work and that any reproduction or use in any form or by any means whatsoever is prohibited without the written consent of UM having been first had and obtained;
(6) I am fully aware that if in the course of making this Work I have infringed any copyright whether intentionally or otherwise, I may be subject to legal action or any other action as may be determined by UM.

    Candidate's Signature   Date:

Subscribed and solemnly declared before,

    Witness's Signature   Date:

Name:

Designation:

ASSESSING REGIONAL LV THICKENING DYSFUNCTION AND DYSSYNCHRONY FOR ACUTE MYOCARDIAL INFARCTION

ABSTRACT

Acute Myocardial Infarction (AMI) is a leading cause of cardiac dysfunction affecting over half a million people worldwide annually. Existing clinical diagnostic and assessment methods could be improved to facilitate early detection and personalized treatment of AMI with the ultimate goal to reduce the associated morbidity and mortality. A 3D personalized LV modelling and thickening assessment framework was developed in this research for assessing regional wall thickening dysfunction and dyssynchrony in AMI patients. A total of 44 subjects consisting of 29 AMI patients and 15 healthy subjects were recruited. Steady-state free precession cine MRI scans were performed for all subjects, and LGE MRI scans were additionally performed for AMI patients. The quantitative spatial thickening measurements across all cardiac phases were computed and correlated against clinical evaluation of infarct transmurality by experienced cardiac radiologist based on AHA 17-segment model and summarized for each individual patient as thickening index (TI) in mm and dyssynchrony index (DI) in % R-R interval. Non-parametric 2-k related sample-based Kruskal-Wallis test was performed to identify significance in thickening and time-to-peak measurements between non-infarcted segments and infarcted segments. Mann-Whitney U test was used to assess TI and DI significance between healthy subjects and AMI patients. The results showed that healthy LV wall segments undergo significant wall thickening ($p<0.05$) during ejection and have on average thicker wall (8.73 ± 1.01 mm) compared with infarcted wall segments (2.86 ± 1.11 mm). Myocardium with thick infarct (i.e. >50% transmurality) underwent remarkable wall thinning during contraction (TI = 1.46 ± 0.26 mm) as opposed to healthy myocardium (TI = 4.01 ± 1.04 mm). For AMI patients, LV which shows sign of thinning

were found to be associated with significantly higher percentage of dyssynchrony as compared to healthy subjects (DI = 15.0 ± 5.0% vs. 7.5±2.0%, p<0.01). Also, strong correlation was found between TI and left ventricular ejection fraction (LVEF) (r=0.892, P<0.01), and moderate correlation between DI and LVEF (r=0.494, P<0.01). The regional wall thickening and dyssynchrony indices extracted from the proposed framework have shown to highly correlate with infarct severity, therefore suggestive of possible practical clinical utility.

Keywords: Myocardial infarction, regional thickening, cine MRI, left ventricle modelling, wall thickness, dyssynchrony.

MENILAI DISFUNGSI PENEBALAN REGIONAL DAN DISINKRONISASI VENTRIKEL KIRI BAGI INFARKSI MIOKARDIUM AKUT

ABSTRAK

Infarksi miokardium akut (AMI) adalah punca utama disfungsi jantung yang menjangkiti setengah juta orang di seluruh dunia setiap tahun. Diagnostik klinikal yang sedia ada dan kaedah-kaedah penilaian boleh dipertingkatkan bagi memudahkan pengesanan awal dan rawatan peribadi dengan matlamat muktamadnya untuk mengurangkan morboditi dan kematian yang berkaitan dengan AMI. Sebuah rangka kerja model peribadi ventrikel kiri (LV) 3D telah direkacipta dalam kajian ini bagi menilai disfungsi penebalan dinding regional dan disinkronisasi yang terdapat di antara pesakit-pesakit AMI. Sejumlah 44 orang subjek yang terdiri daripada 29 pesakit-pesakit AMI dan 15 orang sihat telah direkrut. Pengimbasan "steady-state free precession cine MRI" telah dijalankan pada semua subjek, dan pengimbasan tambahan "LGE MRI" juga dijalankan pada pesakit-pesakit AMI. Pengukuran penebalan spatial secara kuantitatif yang merentasi semua fasa-fasa jantung telah dijana dan dikolerasi dengan penilaian klinikal transmural infarksi oleh perunding radiologi yang berpengalaman berdasarkan AHA 17-segmen model dan pengukuran daripada setiap pesakit AMI dilambangkan dengan pengunaan indeks penebalan (TI) dalam unit mm dan indeks disinkronisasi (DI) dalam unit % selang R-R. Ujian "2-k related sample-based Kruskal-Wallis" yang bukan parametrik telah dilaksanakan untuk mengenal pasti perbezaan penebalan dan pengukuran "time-to-peak" antara segmen bukan infarksi dan segmen infarksi. Ujian "Mann-Whitney U" pula digunakan untuk menilai perbezaan TI dan DI antara orang sihat dan pesakit-pesakit AMI. Hasil kajian inin menunjukkan bahawa segmen LV yang sihat jelas menonjolkan penebalan dinding (p<0.05) semasa ejeksi dan mempunyai purata ketebalan dinding yang lebih tinggi (8.73±1.01 mm) daripada segmen dinding infarksi (2.86±1.11 mm). Miokardium yang memounyai infarksi tebal (iaitu >50% transmuraliti)

menunjukkan penipisan dinding yang luar biasa semasa pengecutan (TI = 1.46±0.26 mm), ini adalah bertentangan dengan miokardium sihat (TI = 4.01±1.04 mm). Di kalangan pesakit-pesakit AMI, LV yang menunjukkan tanda penipisan didapati berkolerasi dengan peratusan disinkronisasi yang lebih tinggi berbanding dengan orang sihat (DI = 15.0 ± 5.0% vs. 7.5±2.0%, p<0.01). Selain itu, kolerasi yang kuat juga didapati antara TI dan fraksi ejeksi ventrikel kiri (LVEF) (r=0.892, P<0.01), dan korelasi serderhana didapati antara DI dan LVEF (r=0.494, P<0.01). Indeks-indeks penebalan dinding regional dan disinkronisasi yang diestrak daripada cadangan rangka kerja ini telah menunjukkan kolerasi yang tinggi dengan keterukan infarksi, oleh itu dicadangkan kemungkinannya dalam penggunaan praktikal klinikal.

Kata-kata kunci: infarksi miokardium, penebalan regional, cine MRI, model ventrikel kiri, ketebalan dinding, disinkronisai.

ACKNOWLEDGEMENTS

TABLE OF CONTENTS

LIST OF TABLES

LIST OF SYMBOLS AND ABBREVIATIONS

AMI : Acute Myocardial Infarction

MRI : Magnetic Resonance Imaging

LGE : Late Gadolinium Enhancement

LV : Left Ventricle

2D : Two-dimensional

3D : Three-dimensional

HCM : Hypertrophic Cardiomyopathy

ES : End-systole

ED : End-diastole

TI : Thickening Index

DI : Dyssynchrony Index

SD : Standard Deviation

AHA : American Heart Association

ECG : Electrocardiogram

EDT : Euclidean Distance Transformation

AAM : Active Appearance Models

nWT : Normal-based Wall Thickness

MDCT : Multidetector Computed Tomography

2D-TTE : Two-dimensional Transthoracic Echocardiography

CT : Computed Tomography

LVEF : Left Ventricle Ejection Fraction

ESV : End-systolic Volume

EDV : End-diastolic Volume

WMSI : Wall Motion Score Index

RV-LV	:	Right Ventricle-Left Ventricle
EWA	:	Expectation Maximization Weighted Intensity Algorithm
CRT	:	Cardiac Resynchronization Therapy
SV	:	Stroke Volume
HDD	:	Hypertensive Heart Disease
°	:	Degrees
Σ	:	Summation
p	:	Probability Value
r	:	Pearson's Correlation Coefficient

CHAPTER 1: INTRODUCTION

Acute myocardial infarction (AMI) is one of the leading causes of morbidity and mortality worldwide (Boateng & Sanborn, 2013; T. H. Lee et al., 1987; Prasad et al., 2010). It occurs when blood supply to the coronary artery is blocked, which causes myocardial tissue injury or necrosis (Prasad et al., 2010). AMI patients were therefore reported to have abnormal left ventricular structure and function (Prasad et al., 2010; Thygesen, Alpert, & White, 2007). In clinical diagnosis, cardiac magnetic resonance imaging (MRI) (van der Geest, de Roos, van der Wall, & Reiber) is considered the gold standard in the evaluation of cardiac anatomy as well as its contractile function (Bhan et al., 2014). In particular, late gadolinium enhancement LGE MRI is the established imaging technique for myocardial viability and infarct quantification (Doltra, Hoyem Amundsen, Gebker, Fleck, & Kelle, 2013) in AMI patients. However, LGE scans have been limited to static analysis at single late post-injection time (Doltra et al., 2013) and do not provide assessment of the degree of functional deterioration, e.g. a reduction in wall motion or thickening dynamics across cardiac cycle.

Standard global measurements such as left ventricle (LV) ejection fraction, volume and mass may not correlate with the local changes of myocardial tissue (Mensel et al., 2014). Regional analysis, therefore, could be useful for the diagnosis and follow up treatment of focal and diffuse myocardial diseases, such as AMI. Current cardiac MRI modalities which employe two-dimensional (2D) in-plane calculation were reported to overestimate LV wall thickness due to its dependency on perpendicular image-to-wall intersection (Beohar et al., 2007; Sheehan et al., 1986; van der Geest et al., 1997). In addition, the 2D analysis did not account for longitudinal shortening which introduces errors when the assessment is performed across phases (Bhan et al., 2014; Holman et al., 1997). To overcome such issues, various efforts in regional assessment resort to three-dimensional (3D) quantification with the use of patient-specific LV models to facilitate

the assessment. Specifically, Holman et al. (1997) employed 3D centerline method to estimate LV wall thickness from cine MRI whereby Beohar et al. (2007) adapted the same technique for looking at myocardial infarction in animal models. This method, however, is prone to overestimating true wall thickness towards the apex due to high curvature of the myocardium. Ordás & Frangi. (2006), by contrast, used normal-based method by computing the distance along the direction of the normal to the endocardial surface from their statistical shape models, aiming towards heart-failure patients to facilitate cardiac resynchronization therapy (CRT) planning. This technique is subject to the same issue faced by Holman et al. (1997) and Beohar et al. (2007), specifically noticeable in cases of localized hypertrophy or myocardial thinning. However, Tobon-Gomez et al. (2010) overcame the issue by demonstrating sphere fitting as a more accurate way to estimate 3D wall thickness from their statistical shape model although they have only used the measurements to distinguish hypertrophic cardiomyopathy (HCM) from hypertensive heart disease, and none on AMI cases. Prasad et al. (2010) opted to use a rather different technique, i.e. Laplace method, to perform 3D motion corrected (Slomka et al., 2007) quantification of regional parameters to institute reference values for wall thickening and wall motion for small groups of different cardiac pathologies and were only qualitatively validated via visual scoring.

Although useful to assess recovery of regional contractile function during follow up treatment, aforementioned studies on regional LV wall thickening analysis (Doltra et al., 2013; O'Regan et al., 2012; Tanabe et al., 2016) have so far been focused on two cardiac phases: end-systolic (ES) and end-diastolic (ED) phases. In AMI patients, however, the maximal changes of regional LV wall thickness do not always occur at these two cardiac phases due to irregular LV wall injury. Also, contractile pattern has reportedly been closely associated with increased risk of heart failure post AMI, suggesting that left ventricle dyssynchrony evaluation could be useful for myocardial infarction prognosis

(Shin et al., 2010). LV wall thickening assessment inclusive of all cardiac phases can provide added information on LV dyssynchrony due to myocardial infarction (Truong et al., 2008). Despite its potential benefits, measuring LV dyssynchrony via 3D wall thickness measurements is only noted in one study using computed tomography (CT) and the assessment was limited to 10 cardiac phases due to lower temporal resolution in comparison to MRI (Tanabe et al., 2016; Truong et al., 2008). Strain imaging remains the most commonly used technique for analyzing LV dyssynchrony (Lamia et al., 2009; Tanabe et al., 2016; Truong et al., 2008), even though it has been shown that dyssynchrony measurements acquired from wall thickness assessment are more reproducible compared to strain analysis (Truong et al., 2008).

In the present study, a novel framework of 3D personalized LV modelling and wall thickening assessment algorithm is developed to evaluate regional cardiac wall thickening dysfunction from base to apex across all cardiac phases. This method takes into consideration motion correction, longitudinal shortening and angular independency in the process. The present study also introduces the utility of thickening index (TI) and dyssynchrony index (DI) based on 3D thickening measurements for each individual AMI patient to reliably assess the severity and track the healing of myocardial contractility functions during follow-up study. The resulting thickening measurements are validated against infarct transmurality and clinical reports.

1.1 Research Objectives

The objectives of this research are as follows:

i. Develop 3D personalized LV modelling and thickening assessment framework for application in AMI patients. This includes the utilization of cine MRI images for 3D reconstruction of the LV and implementation of the sphere

fitting approach to extract 3D LV wall thickness measurements across full cardiac cycle.

ii. Quantify wall thickening dysfunction and dyssynchrony for all AMI patients and compare the measurements against healthy subjects. The proposed thickening and dyssynchrony indices are to be validated with infarct transmurality from LGE scans and clinical reports.

iii. Devise useful 3D visualization and representation method for comprehensive qualitative and quantitative assessment of disease progression in AMI patients.

1.2   Scope of Work

Three distinct phases have been completed for successful implementation of this study. First phase involved the selection of AMI patients and healthy subjects for MRI data acquisition under the strict protocol described by the University Malaya Medical Center.

The second phase of this study focused on developing a 3D modelling cum thickening assessment framework to assess regional LV wall contractility dysfunction and dyssynchrony. In this phase, 3D motion-corrected LV mesh models were reconstructed via slice-to-slice image registration algorithm post semi-automated cine MRI segmentations. Following this, a fully automated 3D wall thickness assessment algorithm was developed to compute and generate color-coded 3D wall thickness models across the full cardiac cycle utilizing the sphere-fitting technique. The 3D wall thickness models were then divided into 17 segments according to the American Heart Association (AHA) standard to faciliate visualization and quantifaction of thickening abnormality and dyssynchrony for all participants in the study. The last steps involved summarizing the LV thickening and dyssynchrony of each patient by the introduction of TI and DI indices.

Finally, the third phase of this study focused towards validating the proposed framework against infarct transmurality from LGE scans and clinical assessment. For this, automatic extraction of infarcted regions and measurement of their transmuralityfrom LGE MRI scans were performed. These measurements were verified against patients reports provided by the radiologists, and then against the regional measurements obtained via the proposed framework.

1.3   Thesis Organization

Chapter 1 delivers the general introduction of this study. It elaborates on the importance of studying AMI and the need to find alternate diagnostic methods. It explains the importance of regional cardiac assessment and its advantage over global measurements, and why current strategies must be improved. It also discusses adversities such as LV dyssynchrony as a result of AMI and what conclusions can be derived from their assessment. Brief comparisons to existing studies are made to further highlight what the present study has contributed to the field.

Chapter 2 is a literature review that provides detailed background of AMI and highlights existing treatment strategies of the disease. It includes a detailed overview of advantages and disadvantages of previous 2D and 3D methods, and different image modalities used to assess AMI and other cardiac conditions. It provides an in-depth analysis of previously conducted regional LV assessments and highlights their recommendations for improving existing diagnostic techniques.

Chapter 3 focuses on detailed explanation of the methodology designed to perform this study. It elaborates on protocol used during data acquisition, the 3D LV modelling cum thickening assessment algorithm, and the validation method. This is followed by a detailed explanation of the statistical tests performed for verification.

Chapters 4 and 5 presents the results and discuss the findings of this research, respectively. Finally, Chapter 6 presents the conclusion of this study and provides recommendation for future work.

CHAPTER 2: LITERATURE REVIEW

2.1   Acute Myocardial Infarction

Cardiac dysfunction has been the leading cause of increased mortality rates affecting over half a million people annually (Boateng & Sanborn, 2013). Acute myocardial infarction (AMI) is considered the most commonly found cardiac diseases (T. H. Lee et al., 1987). AMI occurs when excessive buildup of plaque causes blockade in blood supply to the coronary artery, causing damage to the myocardial tissue (Boateng & Sanborn, 2013). This reduction in myocardial perfusion leads to cell necrosis, which results in deterioration of cardiac performance and heart failure if left untreated. Apart from necrosis, other factors such as coronary artery embolism, hypotension, anemia, and cocaine use are also rare causes of the disease (Boateng & Sanborn, 2013). Furthermore, due to AMI, electrical dysfunction in the form of arrythmias and conduction abnormalities is a common occurrence in most AMI patients. The resulting LV dyssynchrony has a significant impact on ventricular performance (Tanabe et al., 2016). In addition, cardiogenic shock and structural disorders due to LV remodeling, and right ventricle infarction are additional complications that may result post myocardial infarction (Boateng & Sanborn, 2013). Thus, accurate assessment of AMI is essential for effective prognosis and timely recovery

2.2   Imaging Modalities used for AMI diagnosis

This section discusses the most commonly used imaging modalities for AMI application. Computed tomography (CT) has been a common tool used by radiologists to evaluate different levels of tissue densities of all parts of the body (Fred, 2004). In terms of cardiac imaging, CT has been considered a useful tool in identifying coronary anatomy and assessing LV function (Ko, Kim, Park, & Choi, 2014). A CT scanner utilizes x-ray beams to acquire detailed information of body tissues. During CT imaging, the x-ray tube

rotates around the patient to take multiple images from different angles, after which overlapping structures of the body are discarded to make internal anatomy of the region more apparent. However, due to beam hardening artifacts and partial volume-effects, CT based diagnostics of the heart often result in diagnostic dilemma (Nikolaou et al., 2004). Low temporal resolution from CT images has also known to result in poor image quality, yet CT has been used in the past to distinguish abnormal body tissue as it is a faster and presents a more affordable choice when compared to MRI and echocardiography (Ko et al., 2014). This application has been extended to AMI diagnosis, where CT has been used to image AMI patients (Tanabe et al., 2016) to perform strain analysis for LV functional assessment. CT based strain analysis is useful in quantifying extent of LV dyssynchrony post MI. Utility of CT has been justified due to improvements in image resolution, therefore it is the common choice for LV dyssynchrony assessment (Lamia et al., 2009; Tanabe et al., 2016; Truong et al., 2008). Furthermore, even though advances in CT technology include a reduction in x-ray exposure, it has been reported that 40% of collective dose of radiation received annually in patients is due to CT procedures alone (Fred, 2004). Thus, the usage of this modality should be limited due to its unavoidable adversities.

Echocardiography is a medical imaging technique designed specifically to image the heart. Echocardiograms utilize ultrasounds or echoing high-frequency sound waves to generate visuals of the cardiac tissue (Otto, 2012). In recent years, it has been established as an extremely useful diagnostic tool for real time imaging of cardiac dynamics (Lang, Mor-Avi, Sugeng, Nieman, & Sahn, 2006). For example, 2D echocardiography has been reported to have significantly impacted and improved the diagnosis of ischemic heart disease (Lang et al., 2006). The labor intensive and slow reconstructions from average to low resolution 2D echocardiography were primarily utilized for assessing coronary artery disease. With the development of 3D

echocardiography which real-time volumetric imaging, more accurate evaluation of cardiac chambers could be achieved with with an ability to perform localized functional assessment (Lang et al., 2006). Echocardiography has been considered to be suitable for myocardial perfusion imaging along wall motion and wall thickening (Gottdiener, 2003). However, it has been reported to be less sensitive for detecting severity of coronary diseases, including AMI, as compared to nuclear imaging techniquesx (Gottdiener, 2003). In addition, errors due to poor acoustic window and speckle noise have been reported to adversely affect the images acquired from echocardiography (Ko et al., 2014). The imaging technique demands skillful operators as the technique is highly dependent on the radiologist's skills for image acquisition (Bhan et al., 2014). Nonetheless, echocardiography has shown clinical potential for diagnosing functional abnormalities post myocardial infarction (Corona-Villalobos et al., 2016). With adequate skills for data acquisition from 3D echocardiography, high-quality images can be generated to assess functional and regional abnormalities of the myocardium for useful prognosis of AMI.

On the other hand, MRI has been considered a gold standard when it comes to cardiac imaging (Ko et al., 2014). Compared to other imaging modalities such as CT and ultrasound, MRI provides substantially better soft tissue contrast, spatial resolution and image quality, while does not rely on operator skills and is free from ionization radiation (Walsh, Fuster, Fang, & O'Rourke, 2012). In addition, (P. T. Lee et al., 2013) reported that MRI has greater sensitivity towards regional changes in the myocardium when compared to echocardiography. MRI is a complex imaging modality that can be used to acquire data with reference to a variety of acquisition protocols to measure various attributes of the tissue being analyzed (Bitar et al., 2006). One such protocol, the steady-state free precession is the most common for acquisition of 2D+time cine images of the cardiac tissue, due to strong contrast provided between the blood and myocardium. Using MRI, multiple scans are acquired at various LV orientations for structural and functional

assessment of the heart. Apart from the SA scans acquired along the LA, clinical guidelines have recommended the acquisition of LA scans for the 2-chamber view acquired from the center of the mitral valve and through the LV and left atrium, the 4-chamber view which is acquired through mitral and tricuspid valves while cutting through all four chambers of the heart, and the left ventricle outflow tract view, which is acquired through the center of the mitral and aortic valves (Kramer, Barkhausen, Flamm, Kim, & Nagel, 2013). Figure 2.1 depicts the different acquisition views acquired during MRI.
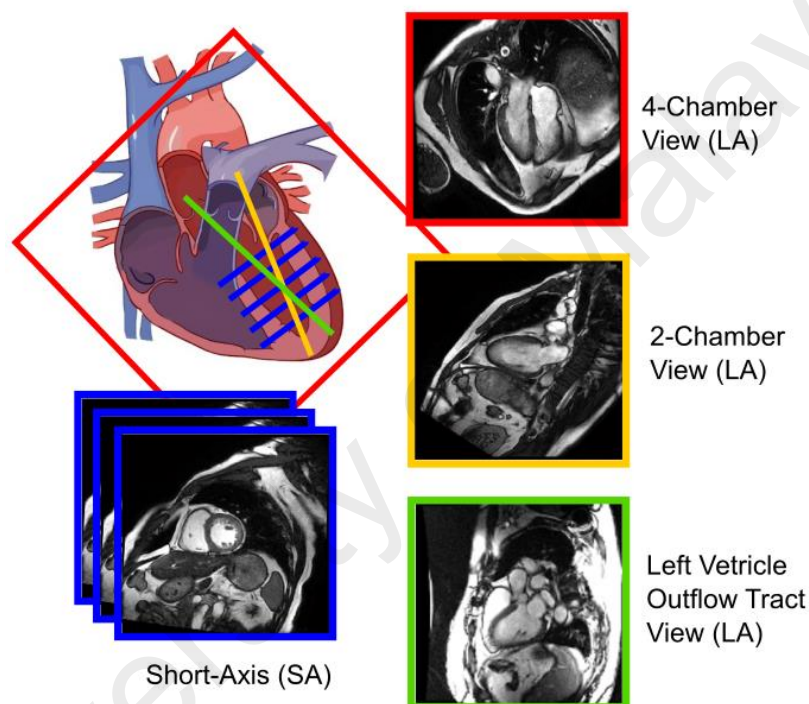
Figure 2.1: Conventional cardiac MRI acquisition views of the LV. (Red) 4-chamber LA view aligned with all four chambers of the heart through the mitral and tricuspid valves. (Yellow) 2-chamber view vertically cutting through the apex and center of mitral valve. (Greenland et al.) LV outflow tract view aligned through the LV and the centers of the mitral and aortic valves. (Blue) SA image stacks across the LV from base to apex.

The delineation of the myocardium walls across the multi-slice images provides quantification of multiple parameters such as: LV end-systolic and end-diastolic volumes, ejection fraction, LV mass, cardiac output, and LV stroke volume. Apart from cine MRI, standard clinical protocol for locating the infarct location and assessing transmurality is performed via the 2D late-gadolinium enhancement (Jahanzad et al.) scans in AMI

patients (Doltra et al., 2013; Jahanzad et al., 2015; Lamia et al., 2009). Gadolinium contrast medium helps distinguish infarcted myocardium from healthy regions in AMI patients, whereby regions of cellular necrosis appear brighter due to increased gadolinium distribution as opposed to healthy myocardium cells which appears dull in appearance as result of lack of contrast medium absorption (Doltra et al., 2013). For example, regions of higher contrast depict infarcted myocardium in Figure 2.2. The impact of infarct on wall motion and cardiac dysfunction can also be assessed from cine and tagged MRI using qualitative visual scoring techniques (Doltra et al., 2013). Nonetheless, it is still the conventional method used to evaluate infarct severity in AMI patients.
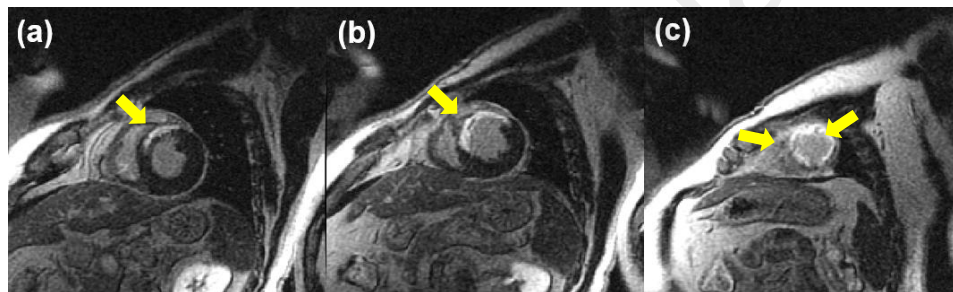
Figure 2.2: The progression of myocardial infarct starting from the basal-anteroseptal region, to the mid-anteroseptal region and extending throughout the apex (indicated by the yellow arrows) is depicted by LGE scans, whereby (a) represents the basal slice, (b) mid slice and (c) apical slice

Furthermore, the cardiac cycle is defined as the period during which the cardiac muscle pumps blood to the body via muscle contractions at the end-systolic phase and muscle relaxation at the end-diastolic phase (Lacey & Lacey, 1978). The cardiac cycle is a vital feature for evaluating cardiovascular performance. Therefore, evaluating these cardiac time frames or cardiac phases of the cardiac cycle would help identify abnormalities in ventricular and valvular performance (Lacey & Lacey, 1978). The cardiac cycle is typically divided in twenty cardiac phases, each depicting a specific phase of the cycle. MRI can produce scans of the cardiac cycle in multiple divisions (Corona-Villalobos et al., 2016). However, most researchers have opted to evaluate ventricular performance post AMI at the end-systolic and end-diastolic cardiac phases when utilizing

MRI due to the strenous and time consuming delineations that accompany while evaluating all twenty cardiac phases (Prasad et al., 2010). Nonetheless, utilization of all twenty cardiac phases would provide extensive detail of the myocardium's funcationality.

Overall, due to the advantages of MRI for regional assessment, many studies have opted to choose MRI over other imaging modalities, especially in AMI applications. In the next section, previous works optimizing the aforementioned modalities using different methods for quantifying regional abnormalities in the myocardium post myocardial infarction are discussed.

2.3   Regional Assessment vs. Global Assessment

Initial evaluation of AMI in local hospitals is currently performed based on clinical history and chest radiographs. This is then followed by electrocardiogram (ECG) assessment for distinguishing the occurrence of non-ST elevation myocardial infarction and ST-elevation myocardial infarction. Global indices are additional quantification measures used to evaluate cardiac performance. Although global indices such as LV ejection fraction, ESV, EDV, LV mass, and cardiac output provide useful insight regarding the extent of deteriorating ventricular function (Boateng & Sanborn, 2013), they do not specifically associate with regional defects of the myocardium (Mensel et al., 2014). For example, Chandrashekara, Mohiaddin, and Rueckert (2004) noted that in some cases global measures exhibited normal readings despite the presence of regional abnormalities in AMI patients. Thus, regional analysis may be more useful for assessing localized abnormalities in the myocardium, especially for AMI patients. In clinical protocol, assessment of myocardial viability and scarring is evaluated using LGE MRI scans. Assessment of infarct severity via 2D LGE MRI scan is reliant on qualitative visual scoring of size and thickness of infarct (also known as infarct transmurality) by radiologist (Doltra et al., 2013). In fact, various image processing methods (Amado et al., 2004; Kim et al., 1999) have been introduced but to date there is no particular threshold treated as a

standard for myocardial scar quantification (Doltra et al., 2013). Current clinical evaluation approaches do not constitute of 3D+time visuals and quantification of regional abnormalities that could facilitate a more comprehensive and accurate assessment of the disease.

Once subjected to AMI, the myocardium undergoes ventricular remodeling, where progressive changes occur in the anatomy of the cardiac wall to retain optimum function in spite of localized injury due to infarction (Gaudron, Eilles, Kugler, & Ertl, 1993; O'Regan et al., 2012; Sutton & Sharpe, 2000; Symons et al., 2014). Recent literature suggests that regional indices such as cardiac wall thickness and changes in wall thickening hold valuable information that can help in diagnosing the extent and location of infarction (Kawel et al., 2012). For instance, it is known that localized injury in the myocardium results in thinning of the cardiac wall at the infarcted regions (Boateng & Sanborn, 2013; O'Regan et al., 2012; Rischpler, 2016). The infarcted regions also show reduced contractility or thickening across the cardiac cycle. The cardiac wall thickness is defined as the thickness of the cardiac wall (in millimeters) that is extracted at any spatial location of the wall during the cardiac cycle. Meanwhile, thickening is the changes of wall thickness from one time point to another, of which the maximal changes normally occur at end-diastole and end-systole in healthy subjects. Literature has shown various studies where accepted values of healthy myocardium and infarcted myocardium thickness are identified (P. T. Lee et al., 2013). Using these values to compare the wall thickness at different regions of the LV, the areas of cardiac wall thinning and contractility dysfunction can be identified to estimate infarct location.

Furthermore, various models have been developed to facilitate regional assessment of the left ventricle, one of which is the American Heart Association's (AHA) 17-segment model (Cerqueira et al., 2002). This model divides the 3D left ventricle in to 17 segments by splitting the LV in to three regions, base, midventricle, and apex. Segment

17 is defined as the tip of the apex, while segments 1 to 6 represent the basal segments, 7-12 represent the midventricular segments, and 13-16 represent the apical segments. Altogether, the 3D 17-segment model facilitates a thorough segmental evaluation of specific segments of the LV, which can be used to map quantifiable data on to 2D bulls-eye diagram, thus making this particular model the preferable choice for left ventricle regional assessment.

There are quite a number of methods proposed to date for assessing regional and global cardiac indices. Earlier methods have employed 2D approaches for quantification, whereas more recent studies have resorted to various 3D approaches. Although these studies provide relevant means for assessment, there are various aspects of the methods that are suggestive of improvement.

2.3.1 Wall thickness and Thickening Acquisition Techniques

The centerline method is the earliest technique proposed by Sheehan et al. (1986) to measure LV wall thickness from imaging data, and has been shown applicable to 2D echocardiography or 2D cine MRI images (McGillem, Mancini, DeBoe, & Buda, 1988; van der Geest et al., 1997). More specifically, this method has been used to measure cardiac wall motion via wall thickness extracted along 100 chords constructed perpendicular to a centerline drawn midway between the epicardial and endocardial wall contours from cine MRI images (Figure 2.3). This study analyzes the relationship between regional and global ventricular function. The study also compares the centerline method with methods that measure motion in predefined regions of the ventricle with respect to accuracy of measuring wall motion abnormalities. Since the analysis is performed in 2D, errors in measurement are incurred due to misalignment of images among various phases and due to longitudinal shortening of LV when progressing through

the cardiac cycle. In addition, the method is prone to overestimating wall thickness due to geometric assumption regarding the myocardium and the imaging plane (Sheehan et al., 1986), which is a limitation of this method highlighted among other works that followed.
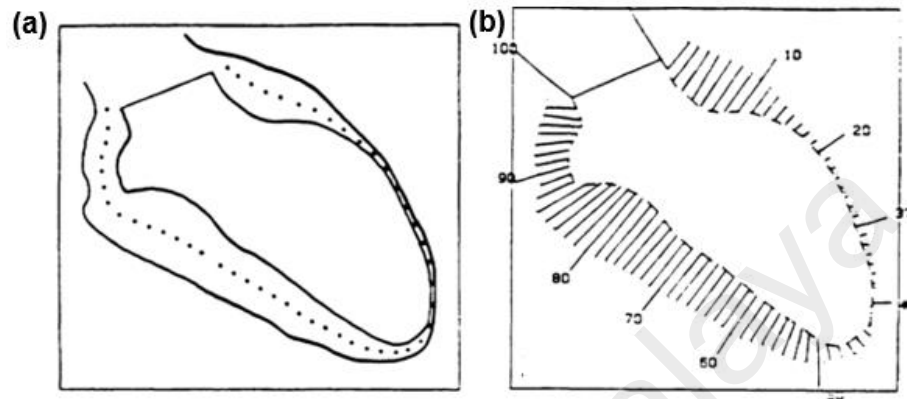
Figure 2.3: Centerline method for regional analysis, where (a) depict the centerline constructed by the computer midway between the endocardial and epicardial contours and (b) where wall motion is measured along 100 chords perpendicularly constructed to the centerline (Sheehan et al., 1986).

Similar to the work of Sheehan et al. (1986), van der Geest et al. (1997) also employed the same method to perform regional quantification of the LV using cine MRI. This study performs 2D centerline method and the modified 3D centerline method and compares the accuracy of both methods, while also providing *in vivo* validation. The study establishes that the 2D centerline approach is based on the assumption that the myocardial wall is always perpendicular to the acquisition plane. However, as acknowledged by Sheehan et al. (1986), this is rarely true since planar 2D methods inevitably overestimate true wall thickness of the LV (Figure 2.4). Therefore, the modified 3D centerline method is developed by this study where overestimation of wall thickness is corrected by acquiring measurements from each chord perpendicular to the myocardium. In addition, with the use of multi-phase cine MRI inclusive of short-axis (SA) and long-axis (LA) images, the resulting 3D wall thickness generated is considered more reliable as opposed to the 2D centerline method. Although the study evaluates the methods reproducibility using phantom studies and healthy subjects, the study does not focus on a particular

disease and rather focuses only on the method's utility in the field. Also, the study does not consider patient motion when it comes to 3D assessment even though slice-to-slice motion is evidenced in portion of the day-to-day clinical acquisition. Similarly, Beohar et al. (2007) has implemented this 3D method to SA and LA cine MRI images to specifically assess acute myocardial infarction, but only in animal models rather than human subjects. The study provided quantification of both wall thickness and wall thickening values and was able to distinguish between normal and infarcted myocardium. However, all the measurements acquired were only from the ES and ED cardiac phases rather than all phases over a full cardiac cycle. Thus, it can be assumed additional improvements can be made to further validate the utility of this approach by providing more comprehensive analysis over the temporal phases of the cardiac cycle.
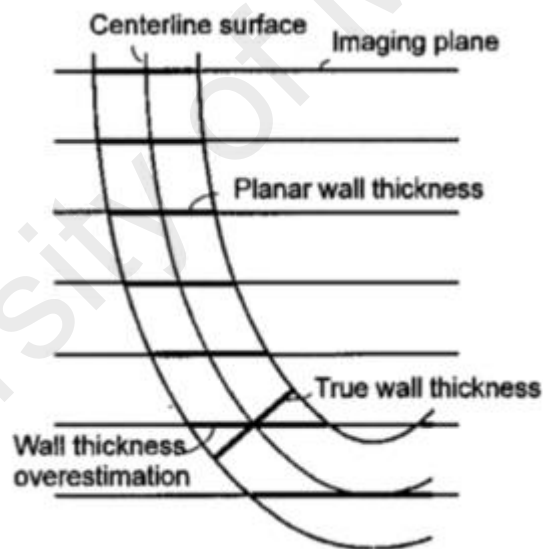
Figure 2.4: Overestimation of wall thickness occurs in SA slices, specifically near the apical region of the LV as the myocardial wall does not intersect perpendicularly with the imaging plane (van der Geest et al., 1997).

Holman et al. (1997) performed quantification of regional LV function using the 3D centerline method for AMI assessment in human subjects. This 3D quantification of wall thickness did correlate with myocardial infarct and the study drew useful conclusions regarding the value of regional assessment for AMI diagnosis. For example, the study's clinical implications suggested wall thinning's association with severely ischemic

myocardium. Nonetheless, the issue of inter-slice misalignment has not been addressed and the study only focused on two cardiac phases (ES and ED). The study therefore has recommended various improvements that may increase the accuracy and reproducibility of the proposed method (Holman et al., 1997).

More recently, Kawel et al. (2012) opted to use 2D centerline method to acquire wall thickness measurements from cine MRI images. As opposed to the aforementioned studies which used manual contouring, in this study the measurements are acquired using semi-automated software tool of QMASS V.7.2 Medis Medical Imaging Systems. Wall thickness was measured on the SA and LA images at the basal, mid-cavity, and apical level in anterior, inferior, lateral, and septal regions. The wall thickness measurements are averaged over 22 to 34 measurements per region and are acquired as 100 measurements per region/slice after contouring of the endocardium and epicardium. However, all the wall thickness measurements are acquired only at the ES and ED for the entire database. Nonetheless, the assumptions of the 2D centerline method remain and the study only provided wall thickness measurements to establish a standard of nominal values of the parameter, instead of applying the method to evaluate different patient groups (Kawel et al., 2012). Figure 2.5 depicts the wall thickness measurements acquired from SA and LA scans via this method.
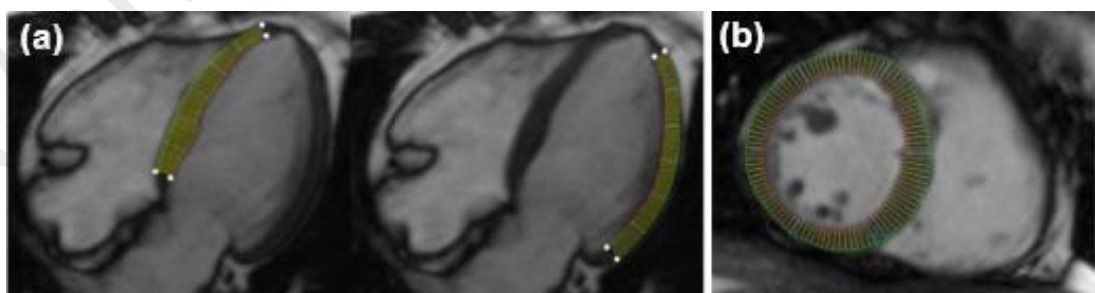
Figure 2.5: Myocardial wall thickness acquired via 2D centerline method at (a) lateral and interior left ventricular wall and (b) SA image. The wall thickness is acquired in 100 measurements per slice for SA image, and 100 measurements per left ventricle wall for LA images after manual contouring of the endocardial and epicardial walls (Kawel et al., 2012).

Moreover, a study in 2010 compared the Laplace's method with Euclidean distance transformation (EDT) method to provide quantification of regional LV parameters such as wall motion and wall thickening. This study considers the limitations of the 3D centerline method prior to utilizing these alternative methods and achieves its objective to quantify standard clinical data using the Laplace's method. Nonetheless, the quantified variables are validated via qualitative visual scoring approach. In addition, two cardiac phases (i.e. ES and ED) are used to acquire wall thickening and wall motion measurements. Although the study does not specifically focus only towards AMI patients, it does establish normal limits for the parameters studied for the normal subjects, which can be used to compare normal values generated from different methods. Also, unlike previous studies, this study performs motion corrections prior to acquiring wall thickness measurements from the cine MRI data. This step is known to significantly reduce errors caused by translational and rotational motions between 2D slices when they were transformed into 3D space (Prasad et al., 2010). Overall, the work of Prasad et al. (2010) suggests the potential of alternative approaches for quantifying regional parameters, as opposed to the planar methods utilized earlier.

A study utilizing a 64-slice multidetector computed tomography (MDCT) conducted measurements of the LV ejection fraction and regional wall motion of a patient population of various cardiac diseases, including AMI (Ko et al., 2014). The study performs regional wall motion analysis by reconstructing multiplanar reformatted images, which are then used to evaluate the SA views at the basal, mid-ventricular, and apical positions along the LA. The analysis is performed via a commercially available software, syngo Circulation. However, the small patient population, and errors due to low temporal resolution from the CT images are suggestive of additional studies for validation and improvement (Ko et al., 2014). Furthermore, other CT-based studies have been used to asses LV dyssynchrony. LV dyssynchrony is a common occurrence post AMI, and the

conventional method to evaluate dyssynchrony is reliant on strain measurements. For example, Tanabe et al. (2016) evaluates the usability of 3D maximum principle strain derived from CT for detecting AMI. However, this study is retrospectively designed and recommends that the 3D maximum principle strain measurements should not be compared to 2D strains such as tagging MRI as not all patients in the study underwent 2D strain analysis. In addition, Truong et al. (2008) used CT to analyze LV dyssynchrony via wall thickness assessment a few years earlier. This study compared dyssynchrony measurements acquired from strain analysis as well as wall thickness assessment and reported the latter to provide more reproducible results. Despite the potential benefits of CT-based regional assessments, the two-dimensional analysis using CT is limited by the low temporal resolution of the imaging modality. In addition, the studies recommended the inclusion of a larger population to validate their findings while also highlighting the drawbacks of ionization radiation exposure from CT (Ko et al., 2014; Lamia et al., 2009; Takx et al., 2012; Tanabe et al., 2016; Truong et al., 2008).

Furthermore, an echocardiography-based study evaluated the effect of wall stress on border and infarct zone geometry (Jackson et al., 2003). For wall thickness measurements, the study utilizes a 2D planar approach whereby three points are identified on the endocardial contours at the ES phase for calculating the distance with respect to the three corresponding and closest points on the epicardial contours. The mean of the three measurements is then extracted to obtain all thickness values. In addition, a study based on speckle tracking echocardiography evaluated left ventricular function and remodeling in a murine model of myocardial infarction (Bhan et al., 2014). This study acknowledges that 2D methods for quantification of regional parameters do not account for longitudinal shortening which is known to have a substantial effect on regional wall thickness measurements when acquired across multiple cardiac phases. While these studies provide useful results, the use of two-dimensional echocardiograms to evaluate

three-dimensional LV is still a relevant concern. In addition, inherent speckle noise, and wall deformation analysis from echocardiography-based studies can be improved to accurately evaluate the infarcted regions of the myocardium (Bhan et al., 2014; Jackson et al., 2003). (Ko et al., 2014) also utilized two-dimensional transthoracic echocardiography (2D-TTE) for regional wall motion assessment in addition to CT, and found the results to be almost identical from both imaging modalities. Although 2D-TTE is used as the reference standard for CT measurements, the study recommended the utilization of MRI in future as it is the established gold standard for volumetric measurements. A more recent study designed for hypertrophy cardiomyopathy patients measures wall thickness by conventional echocardiography and contrast echocardiography on parasternal long axis plane at the basal, mid antero-septal and mid posterior wall. Wall thickness is also extracted from cardiac MRI from SA planes at the ES and ED phases. Upon comparison of the wall thickness measurements, the results provide the conclusion that echocardiography-based risk stratification metrics should not be applied to cardiac MRI; as echocardiography measured higher wall thickness than cardiac MRI in HCM patients (Corona-Villalobos et al., 2016).

2.3.2   3D Modelling Techniques for Regional Assessment

Apart from planar 2D and 3D methods, different research groups have sought towards developing and evaluating the usability of 3D modelling techniques over the last two decades. In this section, we discuss some of these methods to highlight their contribution to this field.

In 2002, Frangi, Rueckert, Schnabel, and Niessen (2002) suggested the utility of statistical shape models for constructing 3D shape models from 2D images. These models have successfully been applied to perform segmentation tasks utilizing landmarks defined

by the user. The statistical shape models are based on a 3D atlas constructed using non-rigid registration. This particular study makes two major contributions. First, it lays out the framework for providing automatic selection of landmarks for 3D shapes to generate statistical shape models. Second, the study extended the generation of shape models by constructing 3D statistical shape models from 3D cardiac MRI. Although this study was the first to utilize 3D statistical shape models to describe the left and right ventricles of the heart via automatic construction of the heart chambers, future investigations are suggested to use multiple cardiac phases if not all for generating the 3D shape models and recommends the improved models can be designed in focus of specific applications.

A few years later, the same research group (Ordás & Frangi, 2006) presented an improved version of their statistical shape models, now referred to as active appearance models (AAMs) with application in quantification of regional parameters. As opposed to their previous work, this study provides full functional analysis of all temporal frames of the MRI study. The automatic quantification approach is used to acquire global indices along with regional parameters inclusive of segmental wall motion, thickening, and dyssynchrony delays. However, the patient population for which the study is performed does not focused on AMI, instead the candidates considered are for cardiac resynchronization therapy. The problem that remains with this study is that the models are generated around a basic shape of an ellipsoid. Although an ellipsoid does represent a rough geometric shape of the LV, it does not accurately represent each aspect of the LV as it is loosely based on the shape of an ellipsoid. Also, additional clinical validation may be required to assess the accuracy of the method to quantify clinical data for other patient types, as this work is verified with hemodynamic evaluation and global cardiac functions.

In 2009, Young, Barnes, Davison, Neubauer, and Schneider (2009) described a fast method for calculation of LV mass and volumes from multiplanar MRI scans. Although the study does not provide quantification for wall thickness, it uses 3D

modelling-based technique to calculate ventricular functions. Current imaging techniques allow the acquisition of 10-20 sections in SA and LA orientations of the LV within clinically accepted time frame of less than 15 minutes. To test the accuracy and efficacy of this 3D method, 15 healthy volunteers, 13 patients with abnormalities due to myocardial infraction, and 8 dogs are studied. The image analysis is conducted via manual contouring and section summation and guide point modeling (GPM) (Figure 2.6). The results highlighted that with the implementation of guide point modeling method, the time required to estimate LV mass, ED volume, ES volume, stroke volume, and ejection fraction was reduced. Although the time saving enables high spatial resolution of multiplanar MR studies of cardiac function to be utilized efficiently in clinical application, the method used does not provide regional quantification of defected myocardium.
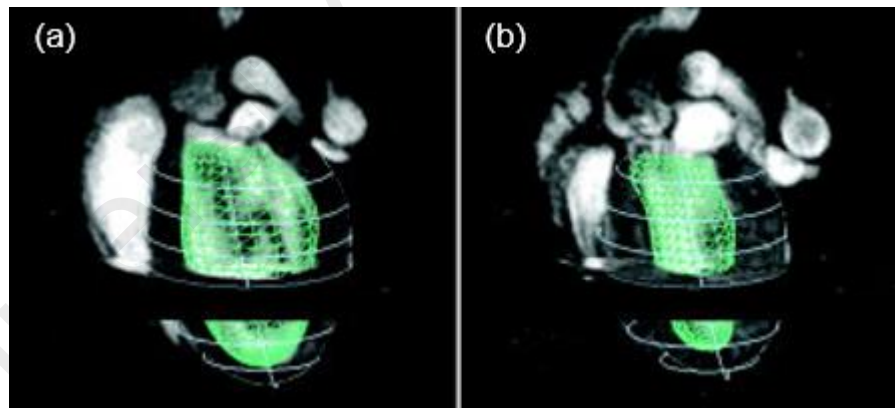
Figure 2.6: Three dimensional models of LV geometry at (a) end-diastole and (b) end-systole via GPM technique. The green frame of the model highlights the endocardial surface and horizontal lines depict the epicardial surface's intersection with the imaging plane (Young et al., 2009).

Furthermore, a 2010 study incorporated a 3D mesh-based wall thickness measurement to differentiate the different phenotypes of LV hypertrophy (i.e. hypertrophy cardiomyopathy and hypertensive heart disease) using cardiac MRI (Tobon-Gomez et al., 2010). This study conducts a comparison between two different techniques

to distinguish the more accurate method for extracting wall thickness of the LV in 3D for differentiating LV hypertrophy. One technique is the normal based wall thickness (nWT) measurement, where the distance from each endocardial point to the epicardial surface is calculated at the normal of endocardial surface. Unfortunately, this technique leads to an overestimation of the infarct size. On the contrary, the medial surface-based technique implemented in this study uses sphere fitting to extract wall thickness. The results showed that maximally inscribed sphere between the set of points on the endocardial and epicardial surface could provide a more accurate estimation of the wall thickness in 3D. Overall, this study overcame the issues of overestimating wall thickness but the technique has yet to be implemented for patients diagnosed with AMI.

In contrast to other studies discussed, only Prasad et al. (2010) has utilized motion correction algorithms (Slomka et al., 2007) prior to wall thickness measurement via the Laplace's method to reduce errors caused by motion artefacts. Similarly, Liew et al. (2015) also identified the need for motion correction of multi-slice MRI data for 3D reconstruction of LV model in an effort to achieve more accurate and reproducible assessment of left ventricular functions in 2015. Specifically, this study incorporates multi-slice image registration into 3D model reconstruction for 10 patients and 10 healthy individuals. Multi-breath hold SA and radial LA images are acquired for each patient. The study improved the reproducibility of various clinical functional measures and concluded that a single time frame is sufficient for motion correction. Also, the study pointed out that integrating more LA slices can improve registration, reproducibility and model reconstruction accuracy for better functional quantification; primarily for data with excessive motion artefacts. Figure 2.7 represents this study's motion corrected LV. Although the motion corrected LV models were not used for regional quantification, the study found substantial accuracy of the motion corrected LV model and suggests its potential for regional analysis (Liew et al., 2015).
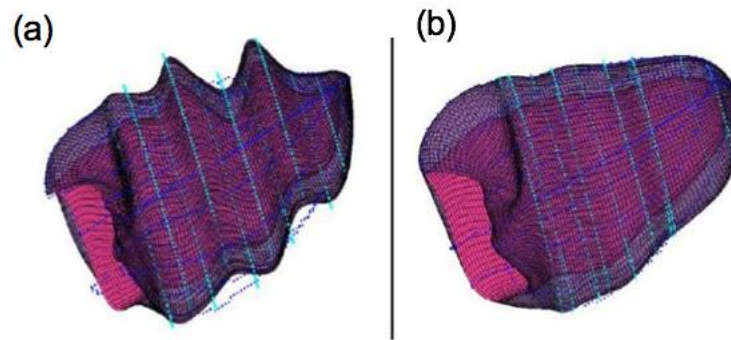
Figure 2.7: Reconstructed 3D surface geometries of the LV of a normal subject after motion corrections. (a) Represents the 3D LV mesh model before registration and (b) depicts the 3D LV mesh model after registration (Liew et al., 2015).

Although 3D modelling provides various advantages over 2D methods, the fact that 3D models are still viewed in 2D plane of a screen, give room to more advanced approaches. Specifically, with the increasing popularity of 3D printing, currently multimodality modelling approach to create 3D printed models for providing direct information of the anatomy and morphology of the cardiac tissue for various purposes including congenital cardiac surgery are becoming popular (Kiraly, 2018). It is highlighted that with using various 3D modelling approaches, the generation of 3D printed anatomical models of individual patients can take personalized diagnosis to newer heights. For example, providing clinicians with better understanding of anatomical features, assist in preoperative planning for cardiac surgery, and for the purpose of manufacturing prostheses. Thus, with the most accurate 3D modelling techniques, 3D printed models of the heart are the long-term application. This only emphasizes the importance of creating the most accurate and reliable 3D models of the heart from 2D scans (Kiraly, 2018).

Overall, there are various studies that have attempted to provide quantification of regional LV parameters and developed 3D models for facilitating visual comprehension of the LV. All in all, the studies collectively made essential contributions while

highlighting various methodologies that can be improved to provide better and more technologically capable methods, specifically for AMI diagnosis.

2.4   Summary and Conclusion

Although the limitations highlighted by previous studies have been briefly discussed in the previous sections, here we summarize the most relevant and common drawbacks of previously proposed methods for regional quantification of LV for functional assessment. First, 2D centerline method implemented is prone to error when the imaging plane does not intersect the cardiac wall orthogonally, which is a rather common problem as the LV is known to be concave and may become deformed in shape under disease conditions (Beohar et al., 2007; Sheehan et al., 1986; van der Geest et al., 1997). Next, longitudinal shortening of LV as evident across cardiac phases has not been accounted for in 2D methods, consequently affecting the accuracy of the myocardium's wall thickness measurements (Bhan et al., 2014; Holman et al., 1997). Also, even with the implementation of 3D centerline (Frangi et al., 2002; Ordás & Frangi, 2006) and normal-based (Tobon-Gomez et al., 2010) methods, it has been found that overestimation of wall thickness is still a concern, which however can be reduced with implementation of sphere fitting approach (Tobon-Gomez et al., 2010). Moreover, although the contributions made by previous studies are in no doubt noteworthy, the results can be further validated and improved with the addition of a larger patient database and an analysis including all phases of the cardiac cycle, as opposed to only the ES and ED phases (O'Regan et al., 2012; Prasad et al., 2010). Also, current 3D models can be further improved to provide a more comprehensive overview of the LV by mapping to bull-eyes diagram with accurate qualitative and quantitative correlation to regional abnormality in the myocardium.

The limitations recognized in existing diagnostic strategies of AMI have been clearly highlighted in earlier works. In the present study, various aspects such as the need

for a more comprehensive visual characterization of the LV for better evaluation of regional abnormalities, as well as the need to perform regional assessment utilizing the full cardiac cycle are taken into consideration. In addition, implementing motion corrected 3D image registration method to develop LV mesh models for wall thickness acquisition via in-house algorithm employing the sphere fitting technique is the prime goal. Earlier works focused on AMI have lacked in providing sufficient clinical data backing up their findings, the present study hopes to provide this validation by correlating its findings to infarct transmurality.

CHAPTER 3: METHODOLOGY

3.1 Study Population

Twenty-nine AMI patients and 15 healthy subjects were recruited in this study. Table 3.1 depicts the demographics and characteristics of all participants. The healthy subjects had no history of cardiovascular disease and had normal cardiac function as determined by echocardiographic assessment. Patients with unstable angina, atrial fibrillation and tachycardia were excluded. The study scan was conducted at the University of Malaya Medical Centre and the imaging protocol was approved by Institutional Ethics Committee (989.75). All participants had provided written informed consent prior to the scanning procedure.

Table 3.1: Subject demographics and characteristics

	Patients ($n = 29$)	Healthy Subjects ($n = 15$)
Gender (male: female)	28:1	9:6
Age	58±7	51±6
Cardiac Function		
LVEF (%)	40±13	65±6
Stroke Volume (%)	68±12	85±19
ESV (%)(Beohar et al.)	117±55	48±16
EDV (%)	183±55	133±30
LV Mass (g)	127±25	89±25
Wall Motion Score Index	2.0±0.4	1.0
Risk Factors (%)		
Dyslipidemia	58	-
Hypertension	62	-
Smoking	52	-
Diabetes	62	-

LVEF = Left Ventricular Ejection Fraction; ESV = End Systolic Volume; EDV = End Diastolic Volume; WMSI = Wall Motion Score Index (which equals to the sum of individual segmental wall motion scores divided by the total number of LV segments, whereby the score of 1: normal, 2:hypokenesis, 3: akinesis and 4:dyskinesis) (Klein et al., 2009).

3.2 MRI Data Acquisition Protocol

All cine and LGE MRI images were acquired during end expiration breath-hold using a 1.5T MRI system (Sigma HDxt 1.5T, GE Healthcare, WI, U.S.A). For each subject, multi-breath-hold steady-state free precession SA cine image stacks covering

from base to apex of the LV were acquired with the following parameters: FOV: 350 × 350 mm, image matrix: 256 × 256, pixel size: 1.37 × 1.37 mm, slice thickness: 8 mm, slice gap: 0 mm, TE/TR: 1.6/3.7ms, flip angle: 55°, number of slices: 10–15, number of cardiac phases: 20, breath-hold time: 15 s. A set of 6 multi-breath-hold LA cine images radially oriented around the center of the LV chamber at uniform angular interval were also prescribed with the same acquisition parameters by using the first SA slice at the base for planning.

For AMI patients, collocated SA inverse recovery fast gradient echo LGE MRI images were obtained. Patients were administered 140 lg/kg/min of adenosine infusion for 4 minutes, followed by 20 ml of normal saline flushing for this acquisition. An intravenous injection of gadolinium-based contrast agent at 0.2 ml/kg was subsequently performed for first-pass perfusion. A further 0.2ml/ kg of the gadolinium agent was administered for rest and delayed gadolinium enhancement at 10-minute intervals. Typical delay enhancement imaging parameters were as follows: TE/TR: 3.0/6.0 ms, inversion time: 200–300 ms (depending on null point of normal myocardium), flip angle: 20˚, no gap between planes and breath-hold time: 18 s. The delay time was chosen to yield images in the mid- to late-systolic phase.

3.3   3D Modelling and Wall Thickening Assessment

The proposed 3D modelling cum thickening assessment algorithm is illustrated in Figure 3.1. The algorithm consists of 3 main steps: (3.3.1) Image Segmentation and Reconstruction of 3D LV model; (3.3.2) Development of 3D cardiac wall thickness model; (3.3.3) AHA Model Division for Regional Thickening Analysis.

3.3.1   Image Segmentation and Reconstruction of 3D LV Model

The LV epicardial and endocardial walls in all SA and LA images were extracted semi-automatically from all SA and LA slices using Segment software package (v2.0 R3950; Medviso AB, Lund, Scania, Sweden) (Heiberg et al., 2010). The contouring was performed by using automated border recognition tool and minor manual fixes (Figure 3.1(a)). The papillary muscles were included in the blood pool and excluded from the myocardium. Motion corrected 3D personalized LV models were subsequently reconstructed for each subject across all cardiac phases (Figure 3.1(b)). Specifically, 3D translational and rotational misalignments between SA and LA images due to motion artifacts were corrected using a multi-slice image registration algorithm, whereas the model was reconstructed using B-spline fitting technique. Both techniques were built based on a previous publication (Liew et al., 2015). Each LV model was formed by two quadrilateral meshes consisting of 101 x 101 vertices to represent the endocardial and epicardial walls, respectively.

3.3.2   Development of 3D Cardiac Wall Thickness Model

A fully automated 3D wall thickness measuring algorithm was developed to compute wall thickness measurements across all vertices of the personalized LV models. The algorithm starts with computing the medial surface between epicardial and endocardial meshes. For each vertex on medial surface, a group of five closest vertices were searched respectively in the epicardial and endocardial meshes using k-nearest neighbor technique (Friedman, Bentley, & Finkel, 1977) based on Euclidean distance. With the vertex of the medial surface acts as the centroid, a sphere was fitted (Figure 3.1 (c)) between the 2 groups of endocardial and epicardial vertices using Nelder-Mead Simplex optimization method (Lagarias, Reeds, Wright, & Wright, 1998). The localized wall thickness was subsequently extracted as the diameter of the fitted sphere. This

process was repeated for all vertices of the LV models across full cardiac cycle. To facilitate visualization of thickening abnormality on the 3D LV model, the thickness measurements were color-coded onto the epicardial surface, generating a 3D LV thickness model for each cardiac phase (Figure 3.1(d)).

3.3.3   AHA Model Division for Regional Thickening Analysis

This step involves identifying the orientation of 3D LV thickness models and mapping them to a common space to accurately track thickening across the full cardiac cycle while considering the longitudinal shortening. Specifically, the thickness model was divided based on the standard 17-segment model defined by the American Heart Association (Cerqueira et al., 2002). To do this, a reference central axis of the models was computed. This central axis was defined as the best fit line of all the centroids from the SA epicardial contours at the first cardiac phase after motion correction in Step 1. All the models across phases were subsequently tilted so that the central axis was aligned with the z-axis. The apex (i.e. Segment 17) was then outlined on the model as portion of the LV myocardium below the minimum z-coordinate point of the endocardial wall. The models were then equally divided into basal, mid and apical layers along the long axis (excluding apex). To obtain the horizontal divisions of these layers, the two RV-LV junction points (denoted as P & Q in Figure 3.1(e)) at the mid-ventricular cine slice were picked, forming a triangle with the intersection (denoted as R) of the central axis and the slice. The interior bisector plane of the angle PRQ containing the central axis was then computed and rotated about the central axis to produce 6:6:4 horizontal divisions of the model at basal:mid:apical layers according to the AHA standard (Figure 3.1(e)).

The AHA-divided 3D LV thickness models were subsequently mapped onto bulls-eye diagrams, producing 20 such diagrams per subject (i.e. one for each cardiac phase). To simplify quantitative and visual assessment, the 20 bulls-eye diagrams were

reduced down to 2 diagrams representing: (1) Regional maximum wall thickening across all phases in unit mm (with reference to the end-diastolic phase, i.e. phase with maximum blood volume) whereby negative thickening value refers to thinning and (2) Time-to-peak in unit % of R-R interval, representing the cardiac phase at which maximum wall thickness/thinning occurs along this interval (Figure 3.1(f)). Two indices, namely thickening index (TI) and dyssynchrony index (DI), based on thickness measurements were also introduced to provide an indication of the overall score of myocardium contractility and dyssynchrony. Thickening index (TI) shows the amount of maximal changes in thickness value in mm with reference to the end-diastolic cardiac phase as defined by Equation 3.1:

$$TI(mm) = \frac{1}{17}\sum_{i=1}^{17}(ES_i - ED_i) \qquad (3.1)$$

where i represents the 17 LV segments, and the average end-systolic (ES) and end-diastolic (ED) wall thickness measurements for LV segments are represented by ES_i and ED_i.

Dyssynchrony index (DI), by contrast, highlights the extent of difference in contraction timings among all cardiac segments in % and is defined by Equation 3.2:

$$DI(\%) = \frac{SD}{20_{phases}} \times 100 \qquad (3.2)$$

where SD is the standard deviation of time-to-peak for all 17 LV segments.

The overall algorithm was implemented in MATLAB (vR2012a, Mathworks, Natick, MA) on an Intel(R) Core(TM) i5-3570 CPU @3.40 GHz computer using parallel computing, and the average time to complete the analysis for each subject across the full cardiac cycle was 8-10 minutes.
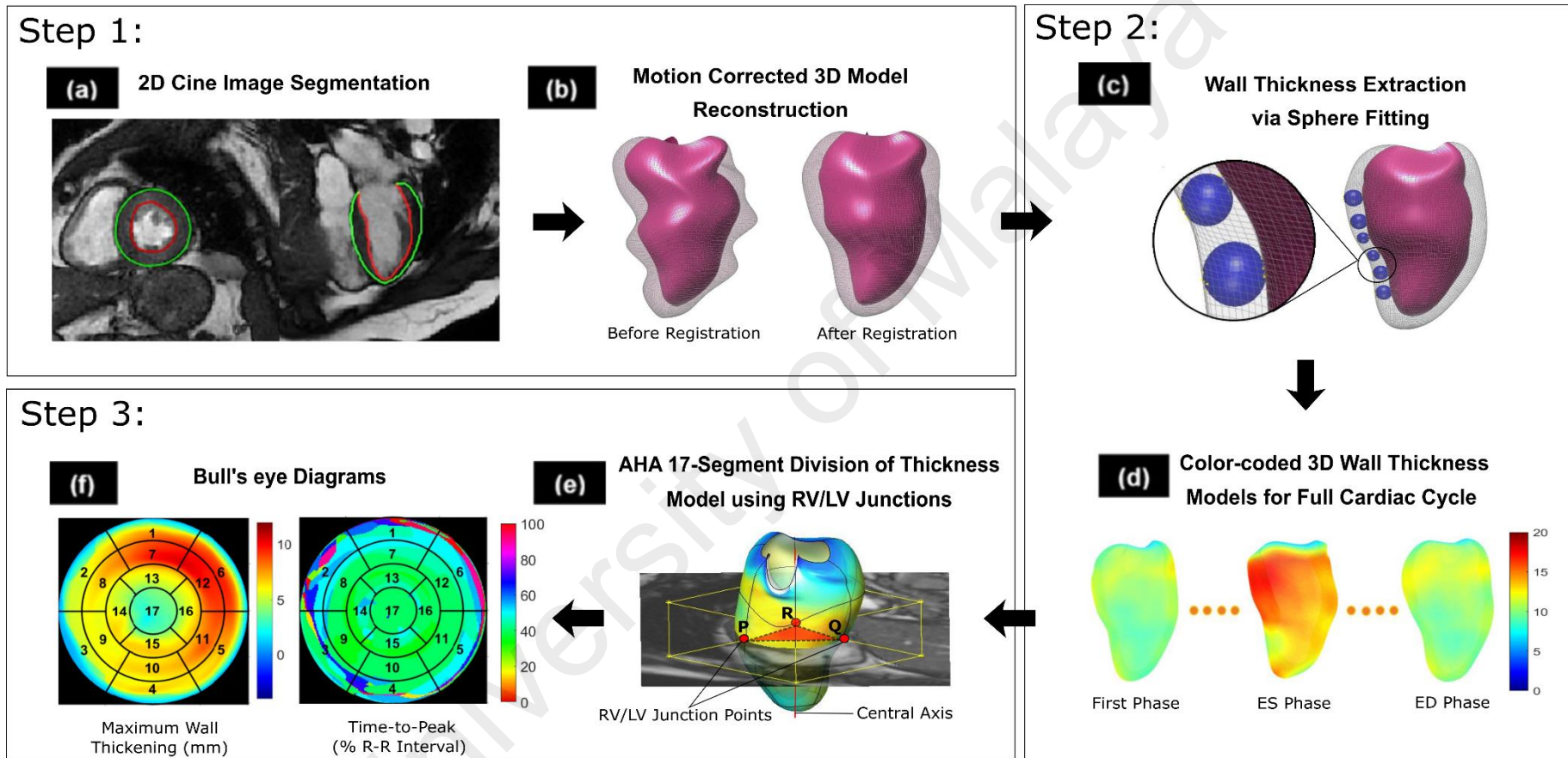
Figure 3.1: Algorithm for 3D modeling cum wall thickening assessment. Step 1: (a) 2D cine SA and LA image are segmented and used to generate the motion corrected 3D LV model in (b) by using multi-slice registration technique. Step 2: (c) Regional wall thickness is extracted via sphere fitting. (d) The resulting color-coded 3D wall thickness models at different cardiac phases. Step 3: (e) The thickness model is divided into AHA 17-segment model based on RV-LV junction points, and (f) the AHA 17-segment model was mapped into bull's eye diagrams for visual and quantitative assessment.

3.4   Validation of Regional Wall Thickening Against Infarct Transmurality

The presence of contrast enhancement in each of the 17 LV segments was quantified from the LGE MRI images of the AMI patients. The quantification involved the extraction of infarct from within the myocardium based on the Expectation Maximization, weighted intensity (EWA), a priori information algorithm (Engblom et al., 2016; Heiberg et al., 2010). The transmurality of infarct in each segment was computed and classified into one of the three categories: (i) 0% (non-infarcted), (ii) 1–50% (non-transmural infarct), and (iii) >50% (transmural infarct) based on the ratio of infarct thickness to LV wall thickness in the radial direction. This quantification was affirmed by the reported infarct location and thickness provided in clinical MRI report as assessed by the radiologist. Regional maximum wall thickening and time-to-peak for various percent of infarct transmuralities were subsequently calculated for validation.

As the data is not normally distributed, non-parametric tests were used to check for significant differences among various groups for comparison: (1) Kruskal-Wallis test (McKight & Najab, 2010) for different categories of transmurality; and (2) Mann-Whitney U test (McKnight & Najab, 2010) for TI and DI between healthy subjects and AMI patients. All statistical analysis was performed using SPSS statistical software (SPSS v24.0; SPSS Inc., Chicago, Illinois, USA).

To visualize the correlation between TI and LVEF, we plotted TI values against LVEF values from all patients while categorizing these patients based on the percentage of transmurally infarcted segments (out of 17 segments). The correlation of TI and DI with LVEF was also determined via Pearson's correlation coefficient, r, with the significance level, p set to 0.05. Blood volumes (end-diastole and end-systole) for the calculation LVEF were obtained from the endocardial mesh of the LV model by surface integration method based on the Divergence Theorem of Gauss (Kreyszig, 2010) which relates the volume of a closed surface to the surface integral.

CHAPTER 4: RESULTS

4.1   Utility of 3D Wall Thickness Models

Mesh models, in its native form (as shown in Figure 3.1(b)), only provide qualitative visual assessment of the changes of LV shape between phases. This visual representation, however, is not sufficiently specific and quantitative to elucidate regional changes of wall thickness for clear identification of regional dysfunction. The 3D modelling cum thickening assessment algorithm developed in this study produces a series of 3D LV models color-coded with localized thickness measurement to facilitate a more comprehensive assessment of regional wall dysfunction from base to apex across all cardiac phases. Figure 4.1 shows the comparison of LV wall thickness in a healthy subject and an AMI patient at every third phase of a full cardiac cycle. The thickness models clearly depict that healthy subject exhibits more uniform pattern of contraction and relaxation along its circumference from base to apex during systole and diastole, respectively. AMI patients, on the other hand, show inhomogeneous thickening pattern where low thickening values were found to coincide with infarct location and severity.
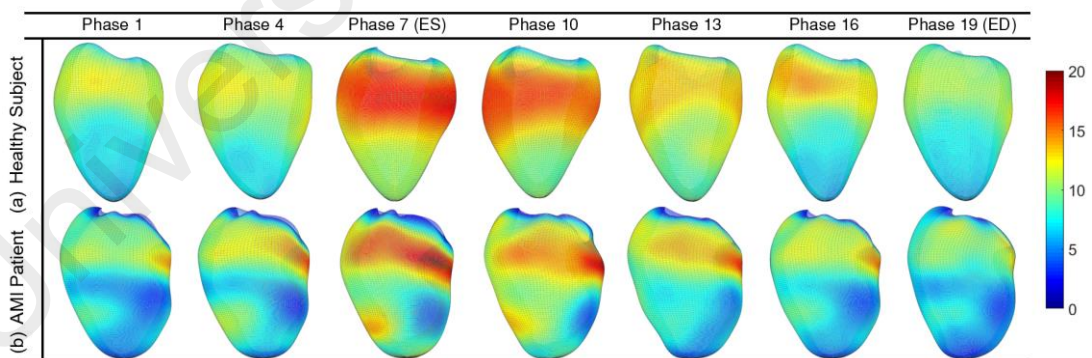
Figure 4.1: Comparison of the 3D cardiac wall thickness models of a healthy subject (a) and an AMI patient (b) at multiple cardiac phases. Color bar represents wall thickness in mm. (ES= end-systolic phase; ED= end-diastolic phase)

Figure 4.2 illustrates that the anomaly in 3D wall thickness measurements correlates well with the transmural infarct depicted by the LGE scan. From the 3D wall

thickness model, the mean wall thickness within the infarcted region for this AMI patient was measured to be 4.5 ± 0.71 mm, which is significantly lower (p<0.01) as compared to the thickness of the healthy region (11.20 ± 0.37 mm). The 3D thickness model provides additional context to cardiac assessment by depicting uniform thickening on the remote regions of the lateral wall as well as the spatial extent of thickening defect across the 3D surface of the septal wall at end-systole due to the presence of infarct, which is currently lacking by merely assessing individual 2D cine and LGE slices.
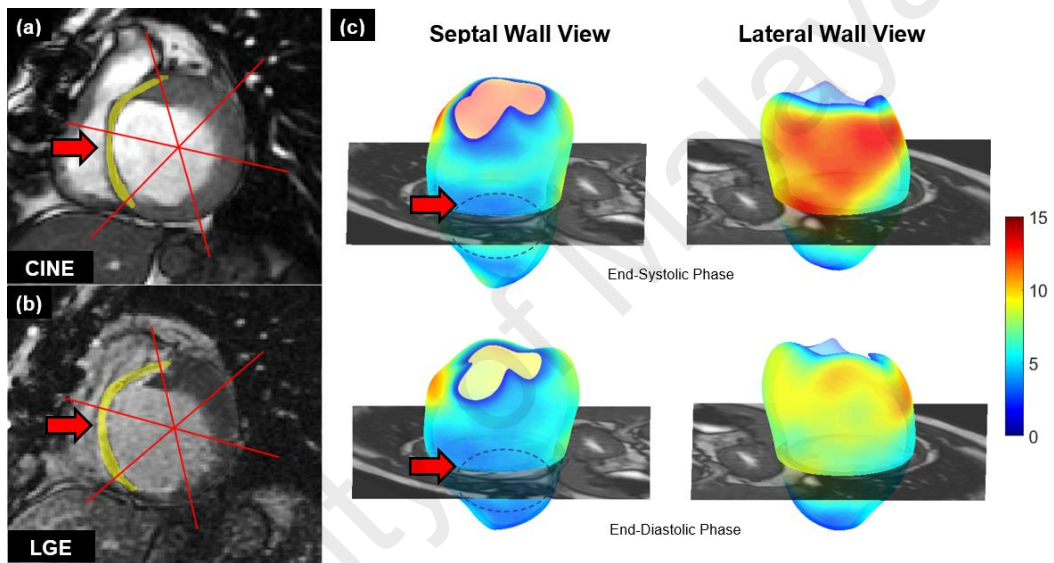
Figure 4.2: Correlation of infarct location on the cine (a) and LGE (b) images with thickness anomaly on the ES and ED 3D wall thickness models (septal wall and lateral wall views) (c). The red arrows are pointing at the same infarcted region of the LV in all images. Yellow shading in (a) and (b) highlight the infarct location. The dark blue region within the circle in (c) highlights the spatial extent of infarct in the septal wall, corresponding to the mid anteroseptal and mid inferoseptal region. Color bar indicates wall thickness in mm.

4.2   Cardiac Performance Evaluation via Wall Thickening and Time to Peak

Figures 4.3 (a) & (b) depict the mean wall thickness profile for each LV segment across full cardiac cycle of a heathy subject in comparison to an AMI patient, whereas Figures 4.3 (c) & (d) shows their corresponding thickening profiles tabulated at basal/mid/apical layers by using our 3D wall thickness modelling method. The thickening profiles define the total amount of thickening with reference to thickness at end-diastolic phase. The AMI patient was diagnosed with multiple transmural infarcts at the base, mid, and apical segments. The thickness profile of healthy subject exhibit a general bell shape which is right skewed and peaked during systolic phase (phase 7 in this case). The corresponding thickening profile at basal/mid/apical layers ((c)) indicates that myocardium at mid-ventricle undergoes greater thickening, followed by apex and base. All the LV segments are shown to thicken in synch in the healthy subject, as indicated by the close proximity in which the segments reach their maximum thickness (i.e. phase 6-8 as indicated by yellow dot markers on the line profiles). This synchronized thickening is also clearly depicted by the thickening profiles (Figure 4.3 (c)) of the basal, mid, and apical layers. For the AMI patient (Figures 4.3 (b) & (d)), by contrast, the thickness profiles of most segments have lost the general bell shape and the LV exhibits less thickening during systole especially at the mid and apical layers. Dyssynchrony is present as the LV segments do not thicken in synch as indicated by the observation that thickness of vast majority of the LV segments peak at different phases across the full cardiac cycle. This lack of thickening and synchronization of all LV segments may have resulted in the lower LVEF and stroke volume (SV) compared with the healthy subject.
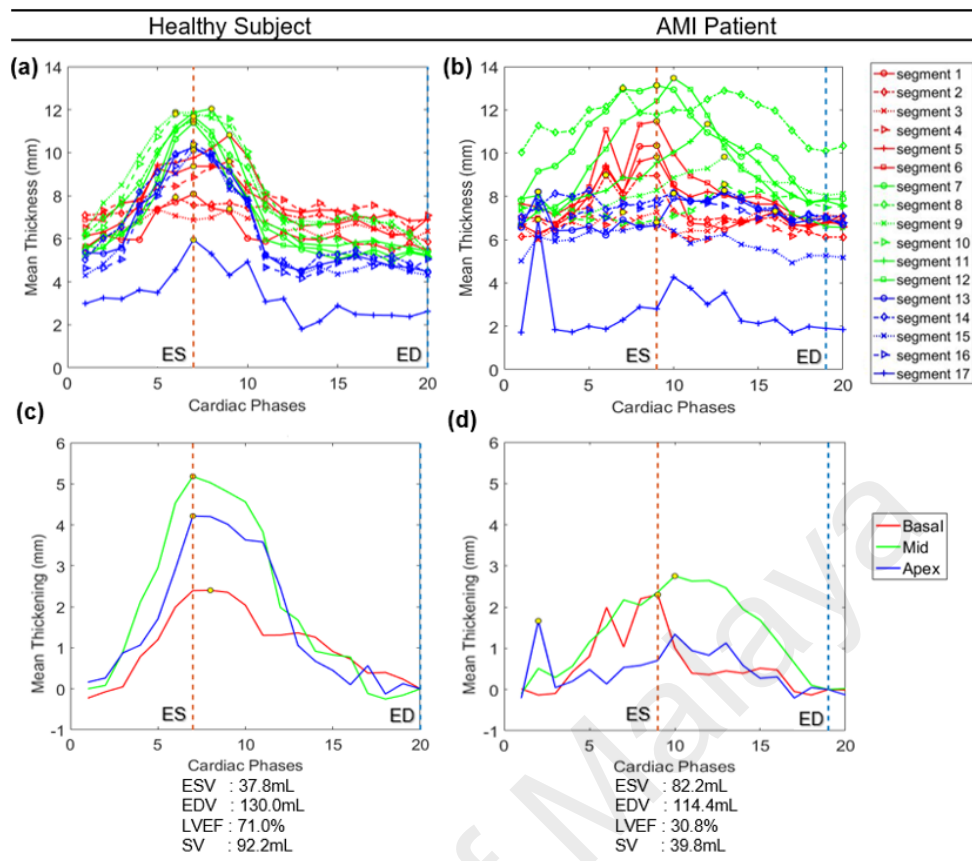
Figure 4.3: Mean segmental wall thickness and thickening profile across the full cardiac cycle for a healthy subject ((a) and (c)), and an AMI patient with multiple transmural infarcts at base, mid, and apex ((b) and (d)). Red profiles – basal segments; green profiles – mid segments; blue profiles – apical segments. The location of peaks of each line profile is indicated by the yellow dot, highlighting the phase at which maximum mean thickness or thickening values were obtained for each segment. ES: end-systole; ED: end-diastole; ESV: end-systolic volume; EDV: end-diastolic volume, LVEF: left ventricular ejection fraction; SV: stroke volume.

Figure 4.4 illustrates the 17-segment bulls-eye diagram of localized maximum wall thickening and time-to-peak for a healthy subject, a patient with moderate myocardial infarction (9/17 of the segments were infarcted), and a patient with severe myocardial infarction (13/17 of segments were infarcted). Healthy subject was observed to attain more uniform maximum wall thickening of approximately 5 to 8 mm (indicated by red-to-orange color in Figure. 4.4 (a) top) primarily at the mid and apical segments, with lateral wall participates more in contraction than septal wall. Most of the segments are also shown to thicken in synch with the maximum thickening achieved at around 25-30% of R-R interval (indicated by green-to-cyan color across majority of the surface area

in Figure. 4.4 (b) bottom). The TI and DI computed for this particular healthy subject is 4.32 mm and 5.8%, respectively.

In contrast, the patient with moderate myocardial infarction has transmural infarction at segments 1, 2, 7, 8, 13, 14, and 17 according to clinical MRI reports (Figure 4.4 (b)). This is in line with the measurements obtained from our 3D wall thickness model, whereby the reduction of maximum wall thickening is observed at these infarcted segments (indicated by cyan in Figure. 4.4 (b) top). The TI value for this patient, nevertheless, is 4.20 mm, which is similar to that of the healthy subject which is observed to be due to noticeably higher thickening values of remote regions in an attempt to maintain normal cardiac function. Hypercontraction of the remote healthy segments is a compensation mechanism to counter the loss of function due to infarction (Jahanzad et al., 2015; Oubel et al., 2012). Besides, delayed thickening is evident at the infarcted segments whereby maximum thickening occurs only at 65-75% of R-R interval in comparison to healthy remote segments at 25-35% of R-R interval (i.e. blue color versus green color in Figure. 4.4 (b) bottom). The degree of dyssynchrony among LV segments is indicated by a higher DI of 8.1%.

Figure 4.4 (c) depicts a patient with majority of the segments are transmurally infarcted except non-transmural segment 8 and remote segments 5, 6, 7, 11 and 12. This patient has a very low TI index score of 1.20 mm. The transmurally infarcted segments appear to be rather static and thicken very little by less than 4 mm over systole. The corresponding time-to-peak plot shows random distribution of color, reflecting highly desynchronized LV segments. The degree of desynchronization is evidenced by high DI score of 18.11%. It appears that even the non-infarcted segments are affected to some extent in terms of time to achieve maximum thickening (mixture of green with other colors).
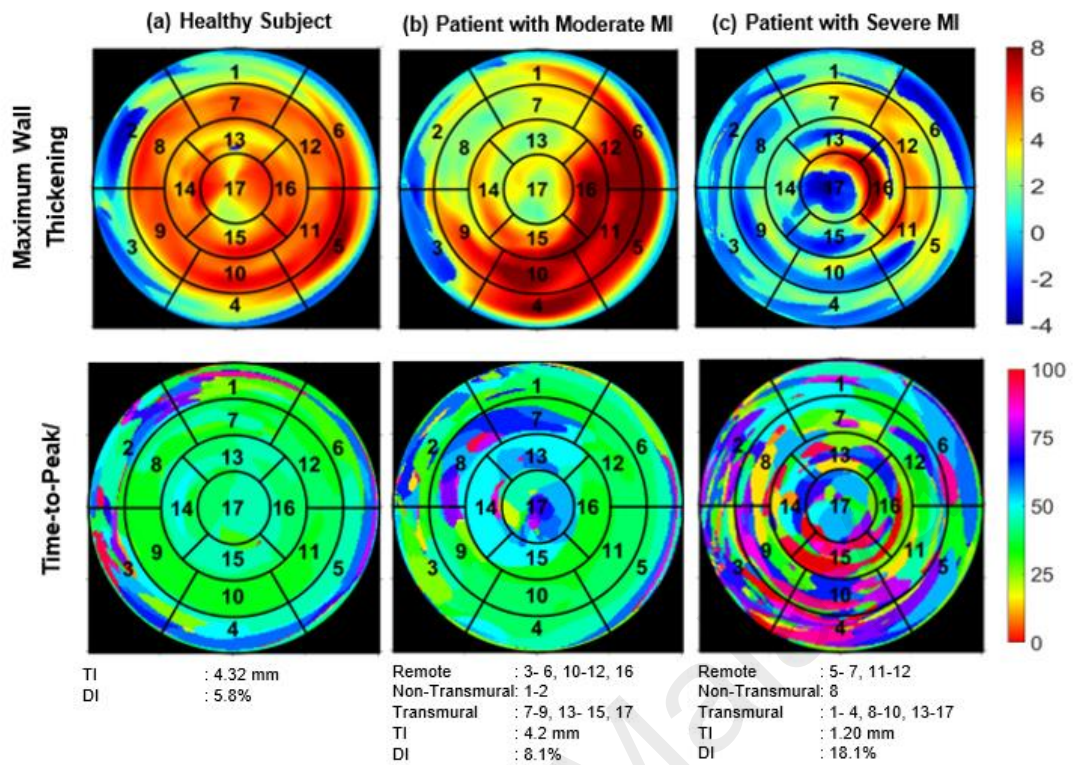
Figure 4.4: Comparison of maximum wall thickening and time-to-peak among (a) healthy subject, (b) patient with moderate myocardial infarction (41% segments infarcted) and (c) patient with severe myocardial infarction (88% segments infarcted). Color bar is in unit mm for maximum wall thickening and in unit % of R-R interval for time-to-peak.

4.3   Statistical Analysis

Figure 4.5 compares the maximum wall thickening (mm) and time-to-peak among control segments (from healthy subjects) and infarcted segments (0%, ≤50% and >50% infarct transmurality) at the basal, mid and apical layers. Altogether, there are 255 control, 245 non-infarcted (0%), 102 non-transmurally infarcted (1–50%) and 146 transmurally infarcted (51-100%) segments. As shown in Figure. 4.5 (a), the maximum amount of thickening at the basal layer is lower as compared to mid and apical layers during systole in healthy subjects. In AMI patient, the non-infarcted segments (0% infarct) seem to have slightly lower maximum thickening than their healthy counterpart. Additionally, a decrease in the maximum thickening is observed with the increase of infarct transmurality: transmural infarct (51% to 100% thickness) in general have lower maximum thickening than the non-transmural infarct (1-50%) at all three layers. Myocardial thinning has also been observed in some infarcted segments, which is suspected due to stretching or pulling by the adjacent healthy regions that were undergoing contraction (Sun & Gravlee, 2012).

For control segments from healthy subjects, maximum thickening occurs at about 40% of the R-R intervals for all layers, which corresponds to systolic phase (Figure. 4.5 (b)). Most of the infarcted segments shown a delay in thickening as well as an increase in the variation of time-to-peak as compared to control segments from healthy subjects. In the presence of infarct in AMI patients, the variation of time-to-peak escalates from non-infarcted, non-transmurally infarcted to transmural infarcted segments. At transmural infarct, the variation recorded in percentage R-R interval was as high as 26.75% at base, 11.35% at mid and 18.05% at the apex in comparison to 7.5% in healthy subjects ($p < 0.05$).
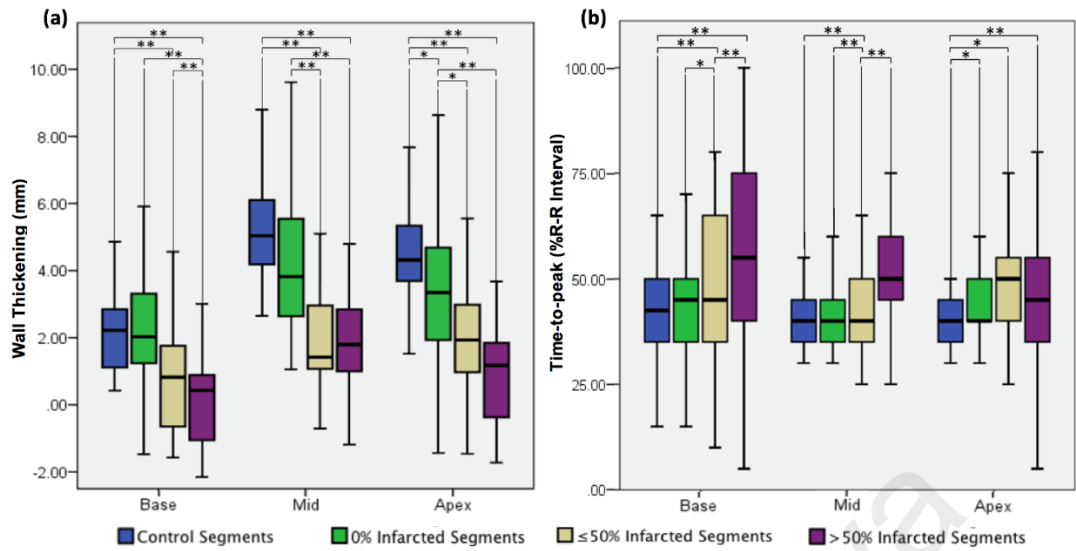
Figure 4.5: Comparison of maximum wall thickening (mm) and time-to-peak among control segment (from healthy subjects) and infarcted segments (0%, ≤50% and >50%) at the basal, mid and apical layers. The box-whisker plot indicates the median, interquartile range, minimum and maximum values (excluding outliers). Significance between groups are indicated by *p<0.05 and **p<0.01.

Table 4.1 highlights that the mean TI across the whole LV of healthy subjects is significantly higher (p<0.01) as compared to the AMI patients (4 mm versus 2.3 mm), indicating the LV of healthy subject thicken more during systole. On the other hand, the mean DI of healthy subjects is 7.5% (corresponds to about offset of 1.5 phase), which is significantly lower (p<0.01) than the AMI patients (i.e. 15% or about 3 phase offset), indicating AMI patients has a higher degree of LV dyssynchrony. The inverse relationship of high thickening value corresponding to low dyssynchrony percentage is evidenced throughout the data.

Table 4.1: Mean thickening index, TI and mean dyssynchrony index, DI for all healthy subjects and AMI patients.

	Mean TI (±SD) mm	Mean DI(±SD) %
Healthy Subjects	4.0(±1.0)	7.5(±2.0)
AMI Patients	2.3(±1.1)	15.0(±5.0)

A good correlation was observed between TI and LVEF, as illustrated in Figure 4.6a. TI score is linearly correlated with LVEF (r=0.892, p<0.01) but inversely correlated with the percentage of segments that are transmurally infarcted. DI, by contrast, only has moderate correlation with LVEF (r = 0.494, p<0.01; graph not shown). Together, both parameters provide evidence of the significant impact transmural infarction has on the deterioration of cardiac functionality. In addition, when compared to the newer method based on feature tracking based wall deformation analysis, although the values were exclusive of segment 17 for all patients, the based radial peak strain measurements also showed good correlation with LVEF (r=0.794, p<0.01), as illustrated in Figure. 4.6b. In spite of this, the TI introduced by the present work showed higher correlation as opposed to radial peak strain. Together, the TI and DI parameters provide evidence of the significant impact transmural infarction has on the deterioration of cardiac functionality.
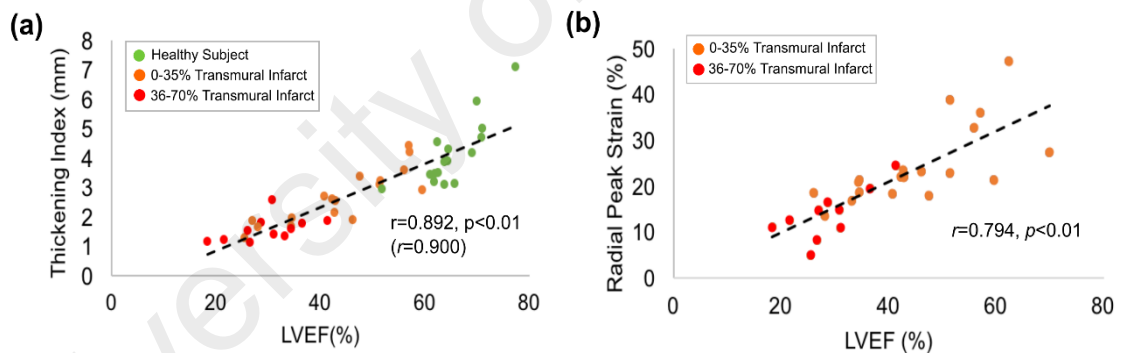
Figure 4.6: (a) Correlation between LVEF (%) and thickening index (mm) for healthy subjects and AMI patients, and (b) correlation between LVEF (%) and radial peak strain (%) for AMI patients. AMI patients were categorized based on different percentage of segments having transmural infarct.

4.4   Variability Study

The Bland–Altman plot for intraobserver variability showed a bias (mean signed difference) of 0.008 mm and limits of agreement of ±0.281 mm in terms of wall thickening (Figure. 8a). Comparing the interobserver variability, the bias was 0.011 mm and the variability in terms of limits of agreement was comparable at ±0.406 mm (Figure. 8b). These results show that the semi-automated segmentation had minimal variation as performed by the interobserver, and even lower variation when performed by the intraobserver, altogether suggestive of this works reproducibility.
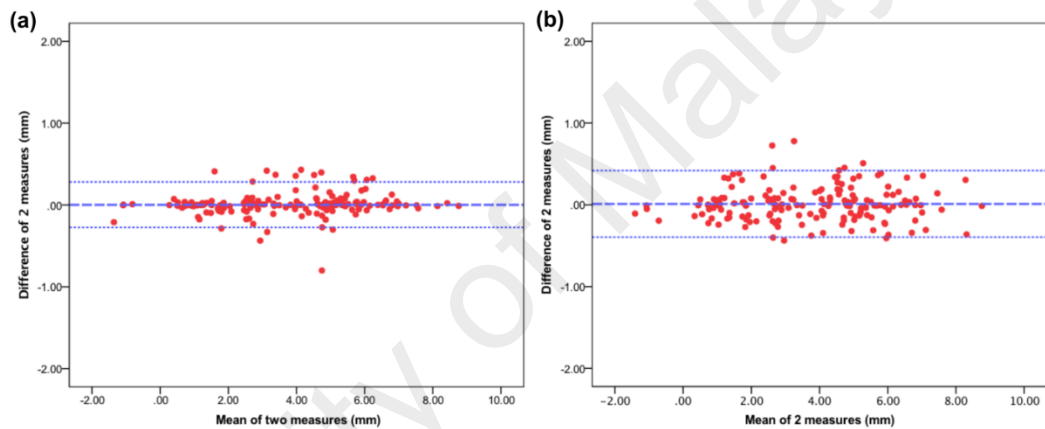
Figure 4.7: Bland–Altman plot analysis of wall thickening values for randomly selected 170 selected thickening values from 5 healthy subjects and 5 patients. (a) Displays the intraobserver pair-comparison and (b) shows interobserver comparison for the data set.

CHAPTER 5: DISCUSSION

In clinical practice, diagnosis of cardiac dysfunction as a result of AMI relies on the assessment of global ventricular functions, along with qualitative visual scoring of infarcted segments using LGE and 2D+time tagged MRI scans (Doltra et al., 2013). This study demonstrates the utility of a 3D personalized LV modelling and sphere-fitting algorithm for the quantitative assessment of regional LV wall thickening from cine MRI scans to identify impaired contractility and dyssynchrony in AMI patients. The TI and DI scores based on 3D wall thickening measurements were introduced and have shown potential in assessing the degree of myocardial injury due to AMI and recovery of wall contractility during follow-up treatment.

In recent years, cardiac shape-related analysis has been increasingly used for longitudinal assessment of cardiac diseases (Ordás & Frangi, 2006; Tobon-Gomez et al., 2010). In comparison to 2D+time visual presentation, 3D+time visuals using 3D personalized modelling presents an added advantage, due to its ability in illustrating the spatial pattern and dynamics of LV characteristics more accurately, especially in the diagnosis and treatment of complex diseases. Despite these advantages, 3D modelling approach is often jeopardized by slice misalignment due to motion artefacts (Liew et al., 2015) (Slomka et al., 2007) caused by various reasons, including the patient's difficulty to breath-hold and stay still during acquisition and arrhythmia. In order to address this issue, motion correction through multi-slice registration approach is performed prior to 3D thickening analysis via sphere fitting technique. In this study, instead of using the two standard LA scans (2-chamber and 4-chamber views), 6 radial LA scans were utilized to aid motion correction and reconstruction of LV model with SA stacks, as a previous study has shown that these additional scans could provide more reproducible cardiac functional measurements (Liew et al., 2015). The acquisition of 6 radial LA slices is considered

feasible in current clinics, as the additional scans only take an extra of 1–2 min over the conventional 2-LA-slice protocol.

Using the sphere-fitting approach, 3D regional LV wall thickness measurements were accurately acquired before being mapped onto bull-eyes diagram to ease visualization and quantitative assessment of spatial thickening pattern and dynamic across full cardiac cycle. Based on current literature, the assessment of spatial thickening pattern and dynamic has yet to be performed utilizing the same algorithm routine which also accounts for longitudinal shortening of LV during ejection. Longitudinal shortening is currently ignored in 2D+time analysis that may introduce errors on assessment of thickening dynamics. In addition, current proposed method is minimally affected by high surface curvature, and less prone to overestimating true wall thickness towards apex as reported for 3D centerline method (Holman et al., 1997). Using the demonstrated 3D approach, the mean wall thickening obtained for healthy subjects was 68.8±15.6% with reference to ED thickness, which is agreeable with previous study using 3D Laplacian technique which recorded healthy mean wall thickening of ≈77% but focused on small groups of various cardiac diseases (Prasad et al., 2010). From this study's 3D analysis of AMI patients, low wall thickness values (<5mm) and in some cases, wall thinning (p<0.01), was observed in infarcted myocardium as opposed to healthy myocardium. As also observed in previously published findings, full thickness infarction was associated with relatively low average wall thickness and deteriorating myocardial functionality (Boateng & Sanborn, 2013; O'Regan et al., 2012). Apart from this, we have observed a direct relationship between increase in transmurality and a decrease in wall thickening and a decrease in synchrony throughout the left ventricle. This is evidenced throughout our patient database whereby segments that have more than 50% myocardial infarction in thickness have depicted the lowest wall thickening values and correspondingly the

lowest synchronization. Therefore, it can be established that the extent of infarct transmurality links both of the metrics introduced in the present work.

In addition, the presented approach clearly depicts that mid and apical segments thicken significantly more during blood ejection than basal segments in the healthy subjects. This is could be for allowing unobstructed blood flow as basal segments are located adjacent to the aortic inflow and outflow tract, and due to shortening of circumferential and oblique myofibers, along with microstructural deformation, which cause wall thickening in the radial direction, thereby contributing to blood ejections (Stöhr, González-Alonso, Bezodis, & Shave, 2013). In the present study, low thickening at infarcted region but hypercontraction in remote regions of several AMI patients was observed. This observation supports the presence of compensatory mechanism to counter loss of function due to AMI, in line with the findings of previous studies (Jahanzad et al., 2015; Oubel et al., 2012). The loss of cardiac functionality in severe myocardial infarction as reported in an earlier study (Pilote, Silberberg, Lisbona, & Sniderman, 1989) is also apparent in this study whereby patients with >35% of the LV segments transmurally infarcted have low blood ejection fraction of 25.8±3.7% as compared to 64.5±5.8% in healthy subjects. These patients were found to have much lower TI of ≤3 mm. The trend of low TI and resulting low LVEF is evident throughout our patients (r = 0.892) and is also likely due to inhomogeneity in the contraction pattern among different LV regions.

This study demonstrates that it is feasible to evaluate LV dyssynchrony of AMI patients based on thickening measurements in order to assess ventricular performance and homogeneity of contractility. Patients with >35% segments transmurally infarcted are noticeably more dyssynchronous with DI score of >15% or >3-phase offset (in comparison to only <7.5% or <1-2 phases offset in healthy subject). Wall thinning is noticeable in some infarcted (non-transmural and transmural) segments during the R-R interval due to stretching by adjacent healthy segments, causing inhomogeneous

contraction. This could be due to severe injury to infarcted myocardium which inflicts segmental variations in activation and contraction timing (Liu et al., 2018). Small regions of cardiac fibrosis in areas of myocardial infarction may also be the culprit for regional inhomogeneity in LV contraction (Liu et al., 2018) as supported by LGE scans, suggesting that cardiac dyssynchrony due to AMI can be accurately quantified from regional wall thickening assessment (Truong et al., 2008).

Ventricular remodeling due to myocardial infarction is a common development among AMI patients (Gaudron et al., 1993). With the evaluation of extent of remodeling, be it adverse or favorable, useful conclusions regarding disease progression, and success or failure of the applied treatment strategy can be made (Symons et al., 2014). However, limited studies have suggested approaches that help facilitate LV remodeling assessment post myocardial infarction. The wall thickening assessment demonstrated in this work offers useful quantification of global as well as regional function, both of which are important in assessing LV remodeling (Bhan et al., 2014). For example, the initial and follow up scan of AMI patients can be compated. This is demonstrated in one patient with myocardial infarction at the mid anteroseptal region and apex in Figure 5.1. An increase in wall thickness and reduced wall thinning at the infarcted segments is observed at 4-month follow-up scan indicating the treatment the patients received has improved his cardiac condition to some extent. The LV segments are also found to contract more synchronously as determined from the much lower DI score of 6.5%) during follow up as compared to initial admission (DI = 10%). There is only subtle improvement of global ventricular performance as observed from LVEF, ESV, and EDV of the patient. In contrast, the 3D wall thickness models and regional thickening diagrams provide additional insights by highlighting the specific regions of the LV that had improved, such as the thickening at the apex and mid anteroseptal segments.
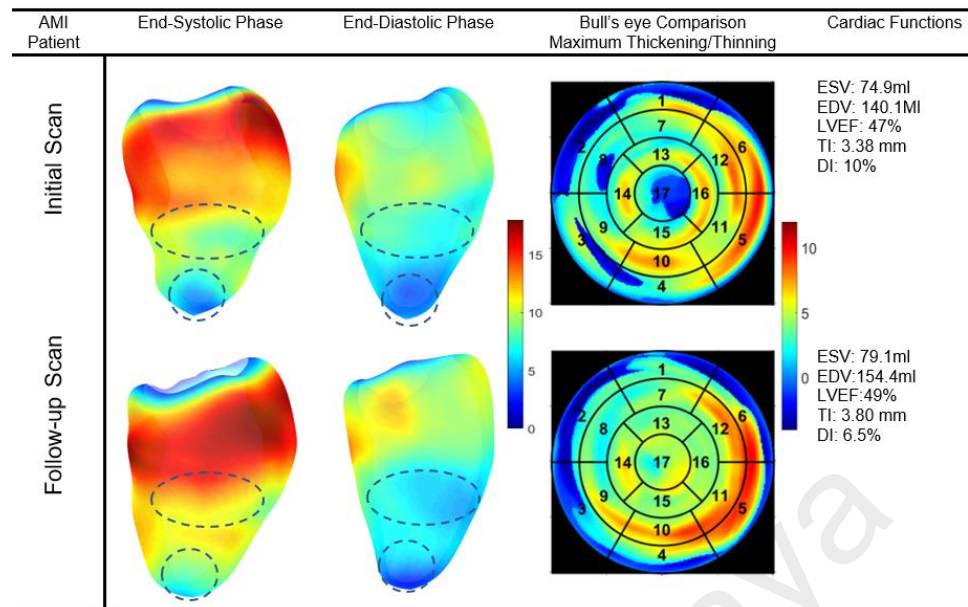
Figure 5.1: Illustrates the 3D wall thickness models and bulls-eye comparison between initial scan and 4 –month follow-up scan of an AMI patient together with global clinical indices.

The present study has two limitations. First, the data acquired is from a relatively small patient population (n=29) and warrant the implementation onto much larger population in order to derive solid conclusion on any clinical finding. Second, semi-automated SA and LA contouring on cine MRI images is performed for reconstructing our motion corrected 3D model. This process can be made more efficient by incorporating fully automated LV segmentation algorithm (Ordás & Frangi, 2006) to the current work flow. Nevertheless, this proof-of-principle study on thickening assessment provides 3D+time representation of contractility useful to aid diagnosis and assess treatment efficacy, therefore suggestive of clinical utility.

CHAPTER 6: CONCLUSION AND FUTURE WORK

6.1   Novelty and Contribution

The framework proposed in the present work stands out due to the incorporation of various aspects that have not been put together in previous studies whilst focusing on a specific patient group. While the framework utilizes the LV mesh model reconstruction and motion correction methods that has been published previously by (Liew et al., 2015)., it has been expanded to incorporate 3D thickness measurements for regional contractility tracking, along with detailed demonstration of the utility of this modelling cum thickness measurement framework on AMI patients. Wall thickness extraction via sphere fitting in in the present work differs from (Tobon-Gomez et al., 2010) due to the difference in the types of mesh model used for fitting. While this work utilizes Euclidean distance of quadrilateral meshes to calculate an approximate medial surface prior to sphere fitting, (Tobon-Gomez et al., 2010) utilizes Voronoi skeletonization of binarized 3D unstructured polygonal LV mesh for its medial surface computation.

In addition, although Bulleye's diagram have been in common use, the source of information was primarily from 2D analysis (Jahanzad et al., 2015), however there was yet to be a method which accomplishes mapping from 3D to Bulleye's diagram to allow 3D+time analysis, which has been done in this work. Such mapping also has the added advantage, allowing longitudinal motion to be accounted for and not ignored as in current 2D analysis therefore reducing errors in tracking the changes of segmental wall thickness from phase to phase.

Finally, this work has introduced the use of thickening and dyssynchrony indices based on 3D regional wall thickness measurement and demonstrated that they could be useful for assessing the severity of AMI patients. Therefore, although each of the steps on their own may have been utilized in one way or another in some works, they have not been used collectively to form a framework for regional assessment of the LV for acute myocardial infarction.

6.2 Conclusion

In conclusion, 3D personalized LV modelling and wall thickening assessment algorithm for quantitative regional evaluation of the spatial distribution and dynamic of LV wall thickening was developed to identify contractility defect and dyssynchrony in AMI patients. The accuracy of this approach for AMI assessment was evidenced by the strong correlation of regional wall thickening (TI) and dyssynchrony (DI) measurements with infarct extent and transmurality as depicted by LGE scans as well as LVEF. By studying the spatial distribution of thickening defect in AMI patients, the results provided 3D visual characterization of progressive LV thickening pattern across a full cardiac cycle and shown evidence of hypercontraction (Jahanzad et al., 2015; Oubel et al., 2012) in remote myocardium. This work could also be used to spatially correlate contractility between initial and follow-up scan for LV remodeling assessment. The work presented has shown potential to be clinically useful and transform existing diagnostic methods by utilizing personalized 3D cardiac modelling for accurate evaluation of regional LV abnormalities in AMI patients.

6.3 Suggestions for Future Work

Since the results have been promising in the present study, in the near future, the aim is to extend the application of regional wall thickening assessment to other diseases. However, prior to doing so, there are specific steps of the methodology that can be further improved in terms of accuracy and time taken to develop the 3D LV wall thickness models. In this section, the specific areas that can be further modified to facilitate other applications, as well as suggested improvements in our methodology for future work are discussed.

6.3.1   Larger Patient Database

In the present study, a total of 44 subjects were used including healthy subjects. Even though validation of the method was provided with these subjects, using a larger patient database in the future could help to further improve current method and further validate the method. For example, with a larger number of healthy subjects the normal values established for wall thickening may be considered more acceptable. In addition, current study is only relevant to AMI diagnosis. The inclusion of patients with other cardiac diseases could be used to prove the utility of current method for regional assessment specific to those conditions.

6.3.2   Fully Automated Image Segmentation

Although the algorithms developed and implemented in the present study, (1) 3D motion corrected LV reconstruction and (2) Wall thickness extraction via sphere fitting, are fully automatic and require no manual user input, the cine MRI segmentation is not completely automatic. The software used to perform semi-automatic segmentations is useful and reasonably accurate in detecting endocardial and epicardial borders in SA image stacks. However, the LA image stacks require additional manual refinements to ensure accuracy of the endocardial and epicardial contours. Although this is not difficult to perform, it does increase the time taken to complete the segmentation of each patient and makes the segmentations subjective to observer variation. With the development of more advanced border and pattern recognition algorithms, fully automatic segmentation on SA and LA image stacks can be implemented. This in turn would significantly improve the time to perform regional assessment of the LV as well as the accuracy of the cine MRI segmentations.

6.3.3   Applications to HCM, HHD and HF Patients

In previous works, the importance of regional assessment for other cardiac conditions has been highlighted, and in some cases even performed. Left ventricular hypertrophy is a complex cardiac condition associated with thickening of the myocardium caused often by either hypertrophic cardiomyopathy (HCM) or hypertensive heart disease (HHD). The segmental thickening values obtained and the TI index introduced in the present study highlights the extent of thickening or thinning in mm relative to regional abnormality due to myocardial infarction. Since the TI is a measure of change in wall thickness, it may find useful application in evaluating disease progression in patients suffering from HCM and HHD.

Cardiac resynchronization therapy (CRT) is an important treatment strategy for heart failure patients. The DI presented in this study provides useful indication regarding the extent of ventricular dyssynchrony in percentage for AMI patients. The application of the DI in this study may be further extended to heart failure patients for evaluating their response to CRT.

REFERENCES

Amado, L. C., Gerber, B. L., Gupta, S. N., Rettmann, D. W., Szarf, G., Schock, R., . . . Lima, J. A. (2004). Accurate and objective infarct sizing by contrast-enhanced magnetic resonance imaging in a canine myocardial infarction model. *Journal of the American College of Cardiology, 44*(12), 2383-2389.

Beohar, N., Flaherty, J. D., Davidson, C. J., Vidovich, M. I., Brodsky, A., Lee, D. C., . . . Sheehan, F. H. (2007). Quantitative assessment of regional left ventricular function with cardiac MRI: Three‐dimensional centersurface method. *Catheterization and Cardiovascular Interventions, 69*(5), 721-728.

Bhan, A., Sirker, A., Zhang, J., Protti, A., Catibog, N., Driver, W., . . . Shah, A. M. (2014). High-frequency speckle tracking echocardiography in the assessment of left ventricular function and remodeling after murine myocardial infarction. *American Journal of Physiology-Heart and Circulatory Physiology, 306*(9), H1371-H1383.

Bitar, R., Leung, G., Perng, R., Tadros, S., Moody, A. R., Sarrazin, J., . . . Nelson, A. (2006). MR pulse sequences: what every radiologist wants to know but is afraid to ask. *Radiographics, 26*(2), 513-537.

Boateng, S., & Sanborn, T. (2013). Acute myocardial infarction. *Disease-a-Month, 59*(3), 83-96.

Cerqueira, M. D., Weissman, N. J., Dilsizian, V., Jacobs, A. K., Kaul, S., Laskey, W. K., . . . Verani, M. S. (2002). Standardized myocardial segmentation and nomenclature for tomographic imaging of the heart: a statement for healthcare professionals from the Cardiac Imaging Committee of the Council on Clinical Cardiology of the American Heart Association. *Journal of the American Society of Echocardiography, 15*(5), 463-467.

Chandrashekara, R., Mohiaddin, R. H., & Rueckert, D. (2004). Analysis of 3-D myocardial motion in tagged MR images using nonrigid image registration. *IEEE transactions on medical imaging, 23*(10), 1245-1250.

Corona-Villalobos, C. P., Sorensen, L. L., Pozios, I., Chu, L., Eng, J., Abraham, M. R., . . . Zimmerman, S. L. (2016). Left ventricular wall thickness in patients with hypertrophic cardiomyopathy: a comparison between cardiac magnetic resonance imaging and echocardiography. *The International Journal of Cardiovascular Imaging, 32*(6), 945-954.

Doltra, A., Hoyem Amundsen, B., Gebker, R., Fleck, E., & Kelle, S. (2013). Emerging concepts for myocardial late gadolinium enhancement MRI. *Current cardiology reviews, 9*(3), 185-190.

Engblom, H., Tufvesson, J., Jablonowski, R., Carlsson, M., Aletras, A. H., Hoffmann, P., . . . Erlinge, D. (2016). A new automatic algorithm for quantification of myocardial infarction imaged by late gadolinium enhancement cardiovascular magnetic resonance: experimental validation and comparison to expert delineations in multi-center, multi-vendor patient data. *Journal of Cardiovascular Magnetic Resonance, 18*(1), 27.

Frangi, A. F., Rueckert, D., Schnabel, J. A., & Niessen, W. J. (2002). Automatic construction of multiple-object three-dimensional statistical shape models: Application to cardiac modeling. *IEEE transactions on medical imaging, 21*(9), 1151-1166.

Fred, H. L. (2004). Drawbacks and limitations of computed tomography: views from a medical educator. *Texas Heart Institute Journal, 31*(4), 345.

Friedman, J. H., Bentley, J. L., & Finkel, R. A. (1977). An algorithm for finding best matches in logarithmic expected time. *ACM Transactions on Mathematical Software (TOMS), 3*(3), 209-226.

Gaudron, P., Eilles, C., Kugler, I., & Ertl, G. (1993). Progressive left ventricular dysfunction and remodeling after myocardial infarction. Potential mechanisms and early predictors. *Circulation, 87*(3), 755-763.

Gottdiener, J. S. (2003). Overview of stress echocardiography: uses, advantages, and limitations. *Current problems in cardiology, 28*(8), 485-516.

Greenland, P., Bonow, R. O., Brundage, B. H., Budoff, M. J., Eisenberg, M. J., Grundy, S. M., . . . Redberg, R. F. (2007). ACCF/AHA 2007 clinical expert consensus document on coronary artery calcium scoring by computed tomography in global cardiovascular risk assessment and in evaluation of patients with chest pain: a report of the American College of Cardiology Foundation Clinical Expert Consensus Task Force (ACCF/AHA Writing Committee to Update the 2000 Expert Consensus Document on Electron Beam Computed Tomography) developed in collaboration with the Society of Atherosclerosis Imaging and Prevention and the Society of Cardiovascular Computed Tomography. *Journal of the American College of Cardiology, 49*(3), 378-402.

Heiberg, E., Sjögren, J., Ugander, M., Carlsson, M., Engblom, H., & Arheden, H. (2010). Design and validation of Segment-freely available software for cardiovascular image analysis. *BMC medical imaging, 10*(1), 1.

Holman, E. R., Buller, V. G., de Roos, A., van der Geest, R. J., Baur, L. H., van der Laarse, A., . . . van der Wall, E. E. (1997). Detection and quantification of dysfunctional myocardium by magnetic resonance imaging: a new three-dimensional method for quantitative wall-thickening analysis. *Circulation, 95*(4), 924-931.

Jackson, B. M., Gorman, J. H., Salgo, I. S., Moainie, S. L., Plappert, T., StJohn-Sutton, M., . . . Gorman, R. C. (2003). Border zone geometry increases wall stress after myocardial infarction: contrast echocardiographic assessment. *American Journal of Physiology-Heart and Circulatory Physiology, 53*(2), H475.

Jahanzad, Z., Liew, Y. M., Bilgen, M., McLaughlin, R. A., Leong, C. O., Chee, K. H., . . . Ng, S.-C. (2015). Regional assessment of LV wall in infarcted heart using tagged MRI and cardiac modelling. *Physics in Medicine & Biology, 60*(10), 4015.

Kawel, N., Turkbey, E. B., Carr, J. J., Eng, J., Gomes, A. S., Hundley, W. G., . . . van der Geest, R. J. (2012). Normal Left Ventricular Myocardial Thickness for Middle-Aged and Older Subjects With Steady-State Free Precession Cardiac Magnetic

ResonanceClinical Perspective. *Circulation: Cardiovascular Imaging, 5*(4), 500-508.

Kim, R. J., Fieno, D. S., Parrish, T. B., Harris, K., Chen, E.-L., Simonetti, O., . . . Judd, R. M. (1999). Relationship of MRI delayed contrast enhancement to irreversible injury, infarct age, and contractile function. *Circulation, 100*(19), 1992-2002.

Kiraly, L. (2018). Three-dimensional modelling and three-dimensional printing in pediatric and congenital cardiac surgery. *Translational pediatrics, 7*(2), 129.

Klein, P., Holman, E. R., Versteegh, M. I., Boersma, E., Verwey, H. F., Bax, J. J., . . . Klautz, R. J. (2009). Wall motion score index predicts mortality and functional result after surgical ventricular restoration for advanced ischemic heart failure. *European Journal of Cardio-Thoracic Surgery, 35*(5), 847-853.

Ko, S., Kim, Y., Park, J., & Choi, N. (2014). Assessment of left ventricular ejection fraction and regional wall motion with 64-slice multidetector CT: a comparison with two-dimensional transthoracic echocardiography. *The British journal of radiology*.

Kramer, C. M., Barkhausen, J., Flamm, S. D., Kim, R. J., & Nagel, E. (2013). Standardized cardiovascular magnetic resonance (CMR) protocols 2013 update. *Journal of Cardiovascular Magnetic Resonance, 15*(1), 91.

Kreyszig, E. (2010). *Advanced engineering mathematics*: John Wiley & Sons.

Lacey, B. C., & Lacey, J. I. (1978). Two-way communication between the heart and the brain: Significance of time within the cardiac cycle. *American Psychologist, 33*(2), 99.

Lagarias, J. C., Reeds, J. A., Wright, M. H., & Wright, P. E. (1998). Convergence properties of the Nelder--Mead simplex method in low dimensions. *SIAM Journal on optimization, 9*(1), 112-147.

Lamia, B., Tanabe, M., Kim, H. K., Johnson, L., Gorcsan III, J., & Pinsky, M. R. (2009). Quantifying the role of regional dyssynchrony on global left ventricular performance. *JACC: Cardiovascular Imaging, 2*(12), 1350-1356.

Lang, R. M., Mor-Avi, V., Sugeng, L., Nieman, P. S., & Sahn, D. J. (2006). Three-dimensional echocardiography: the benefits of the additional dimension. *Journal of the American College of Cardiology, 48*(10), 2053-2069.

Lee, P. T., Dweck, M. R., Prasher, S., Shah, A., Humphries, S. E., Pennell, D. J., . . . Payne, J. R. (2013). Left Ventricular Wall Thickness and the Presence of Asymmetric Hypertrophy in Healthy Young Army RecruitsClinical Perspective. *Circulation: Cardiovascular Imaging, 6*(2), 262-267.

Lee, T. H., Rouan, G. W., Weisberg, M. C., Brand, D. A., Acampora, D., Stasiulewicz, C., . . . Goldstein-Wayne, B. (1987). Clinical characteristics and natural history of patients with acute myocardial infarction sent home from the emergency room. *The American journal of cardiology, 60*(4), 219-224.

Liew, Y., McLaughlin, R., Chan, B., Aziz, Y. A., Chee, K., Ung, N., . . . Lim, E. (2015). Motion corrected LV quantification based on 3D modelling for improved functional assessment in cardiac MRI. *Physics in medicine and biology, 60*(7), 2715.

Liu, S., Guan, Z., Jin, X., Meng, P., Wang, Y., Zheng, X., . . . Yang, J. (2018). Left ventricular diastolic and systolic dyssynchrony and dysfunction in heart failure with preserved ejection fraction and a narrow QRS complex. *International journal of medical sciences, 15*(2), 108.

McGillem, M. J., Mancini, G. J., DeBoe, S. F., & Buda, A. J. (1988). Modification of the centerline method for assessment of echocardiographic wall thickening and motion: a comparison with areas of risk. *Journal of the American College of Cardiology, 11*(4), 861-866.

McKight, P. E., & Najab, J. (2010). Kruskal‑Wallis Test. *Corsini Encyclopedia of Psychology*.

McKnight, P. E., & Najab, J. (2010). Mann‑Whitney U Test. *Corsini Encyclopedia of Psychology*.

Mensel, B., Quadrat, A., Schneider, T., Kühn, J.-P., Dörr, M., Völzke, H., . . . Lorbeer, R. (2014). MRI-based determination of reference values of thoracic aortic wall thickness in a general population. *European Radiology, 24*(9), 2038-2044.

Nikolaou, K., Flohr, T., Knez, A., Rist, C., Wintersperger, B., Johnson, T., . . . Becker, C. R. (2004). Advances in cardiac CT imaging: 64-slice scanner. *The International Journal of Cardiovascular Imaging, 20*(6), 535-540.

O'Regan, D. P., Shi, W., Ariff, B., Baksi, A. J., Durighel, G., Rueckert, D., & Cook, S. A. (2012). Remodeling after acute myocardial infarction: mapping ventricular dilatation using three dimensional CMR image registration. *Journal of Cardiovascular Magnetic Resonance, 14*(1), 41.

Ordás, S., & Frangi, A. F. (2006). *Automatic quantitative analysis of myocardial wall motion and thickening from long-and short-axis cine MRI studies.* Paper presented at the Engineering in Medicine and Biology Society, 2005. IEEE-EMBS 2005. 27th Annual International Conference of the.

Otto, C. M. (2012). *The practice of clinical echocardiography*: Elsevier Health Sciences.

Oubel, E., De Craene, M., Hero, A., Pourmorteza, A., Huguet, M., Avegliano, G., . . . Frangi, A. F. (2012). Cardiac motion estimation by joint alignment of tagged MRI sequences. *Medical image analysis, 16*(1), 339-350.

Pilote, L., Silberberg, J., Lisbona, R., & Sniderman, A. (1989). Prognosis in patients with low left ventricular ejection fraction after myocardial infarction. Importance of exercise capacity. *Circulation, 80*(6), 1636-1641.

Prasad, M., Ramesh, A., Kavanagh, P., Tamarappoo, B. K., Nakazato, R., Gerlach, J., . . . Germano, G. (2010). Quantification of 3D regional myocardial wall thickening

from gated magnetic resonance images. *Journal of Magnetic Resonance Imaging, 31*(2), 317-327.

Rischpler, C. (2016). Acute myocardial infarction. *The quarterly journal of nuclear medicine and molecular imaging: official publication of the Italian Association of Nuclear Medicine (AIMN)[and] the International Association of Radiopharmacology (IAR),[and] Section of the Society of.. 60*(3), 236-251.

Sheehan, F. H., Bolson, E. L., Dodge, H. T., Mathey, D. G., Schofer, J., & Woo, H. (1986). Advantages and applications of the centerline method for characterizing regional ventricular function. *Circulation, 74*(2), 293-305.

Shin, S.-H., Hung, C.-L., Uno, H., Hassanein, A. H., Verma, A., Bourgoun, M., . . . Califf, R. M. (2010). Mechanical dyssynchrony after myocardial infarction in patients with left ventricular dysfunction, heart failure, or both. *Circulation, 121*(9), 1096-1103.

Slomka, P. J., Fieno, D., Ramesh, A., Goyal, V., Nishina, H., Thompson, L. E., . . . Germano, G. (2007). Patient motion correction for multiplanar, multi‑breath‑hold cardiac cine MR imaging. *Journal of Magnetic Resonance Imaging, 25*(5), 965-973.

Stöhr, E. J., González-Alonso, J., Bezodis, I. N., & Shave, R. (2013). Left ventricular energetics: new insight into the plasticity of regional contributions at rest and during exercise. *American Journal of Physiology-Heart and Circulatory Physiology, 306*(2), H225-H232.

Sun, B., & Gravlee, G. (2012). Surgical ventricular restoration and remodeling. *A practical approach to cardiac anesthesia, 4th ed. Philadelphia: Lippincott Williams & Wilkins*, 517.

Sutton, M. G. S. J., & Sharpe, N. (2000). Left ventricular remodeling after myocardial infarction. *Circulation, 101*(25), 2981-2988.

Symons, R., Masci, P. G., Goetschalckx, K., Doulaptsis, K., Janssens, S., & Bogaert, J. (2014). Effect of infarct severity on regional and global left ventricular remodeling in patients with successfully reperfused ST segment elevation myocardial infarction. *Radiology, 274*(1), 93-102.

Takx, R. A., Moscariello, A., Schoepf, U. J., Barraza, J. M., Nance, J. W., Bastarrika, G., . . . Schoenberg, S. O. (2012). Quantification of left and right ventricular function and myocardial mass: comparison of low-radiation dose 2nd generation dual-source CT and cardiac MRI. *European journal of radiology, 81*(4), e598-e604.

Tanabe, Y., Kido, T., Kurata, A., Sawada, S., Suekuni, H., Kido, T., . . . Miyagawa, M. (2016). Three-dimensional maximum principal strain using cardiac computed tomography for identification of myocardial infarction. *European Radiology*, 1-9.

Thygesen, K., Alpert, J. S., & White, H. D. (2007). Universal definition of myocardial infarction. *Journal of the American College of Cardiology, 50*(22), 2173-2195.

Tobon-Gomez, C., Butakoff, C., Yushkevich, P., Huguet, M., & Frangi, A. (2010). *3D mesh based wall thickness measurement: identification of left ventricular hypertrophy phenotypes.* Paper presented at the Engineering in Medicine and Biology Society (EMBC), 2010 Annual International Conference of the IEEE.

Truong, Q. A., Singh, J. P., Cannon, C. P., Sarwar, A., Nasir, K., Auricchio, A., . . . Moccetti, T. (2008). Quantitative analysis of intraventricular dyssynchrony using wall thickness by multidetector computed tomography. *JACC: Cardiovascular Imaging, 1*(6), 772-781.

van der Geest, R. J., de Roos, A., van der Wall, E. E., & Reiber, J. H. (1997). Quantitative analysis of cardiovascular MR images. *The International Journal of Cardiac Imaging, 13*(3), 247-258.

Walsh, R., Fuster, V., Fang, J., & O'Rourke, R. A. (2012). *Hurst's the Heart Manual of Cardiology*: McGraw Hill Professional.

Yamani, H., Cai, Q., & Ahmad, M. (2012). Three‐Dimensional Echocardiography in Evaluation of Left Ventricular Indices. *Echocardiography, 29*(1), 66-75.

Young, A. A., Barnes, H., Davison, D., Neubauer, S., & Schneider, J. E. (2009). Fast left ventricular mass and volume assessment in mice with three‐dimensional guide‐point modeling. *Journal of Magnetic Resonance Imaging, 30*(3), 514-520.

LIST OF PUBLICATIONS AND PAPERS PRESENTED

Conference

- ➡ Khalid A, Chan BT, Lim E, and Liew YM. 3D cardiac wall thickening assessment for acute myocardial infarction. IOP Conference Series: Materials Science and Engineering; 2017: IOP Publishing.

Journal Article

- ➡ Khalid A, Chan BT, Lim E, and Liew YM. Assessing regional left ventricular thickening dysfunction and dyssynchrony via personalized modelling and 3d wall thickness measurements for acute myocardial infarction. Journal of Magnetic Resonance Imaging; 2018.